REPORT DOCUMENTATION PAGE

Form Approved
OMB No. 0704-0188

1. REPORT DATE *(DD-MM-YYYY)*	2. REPORT DATE	3. DATES COVERED *(From - To)*
04-02-2004	Final	31-07-1999-28-02-2002

4. TITLE AND SUBTITLE
Modeling and Control of the ARCP in Power and Drive Systems

5a. CONTRACT NUMBER

5b. GRANT NUMBER
N00014-99-1-1004

5c. PROGRAM ELEMENT NUMBER

6. AUTHOR(S)
Jeffrey Mayer and Heath Hofmann

5d. PROJECT NUMBER
00PR05489

5e. TASK NUMBER

7. PERFORMING ORGANIZATION NAME(S) AND ADDRESS(ES)
The Pennsylvania State University
121 EE East
University Park, PA 16802

20040218 164

N/A

9. SPONSORING/MONITORING AGENCY NAME(S) AND ADDRESS(ES)
Office of Naval Research
Ship Structures and Systems Division
800 North Quincy Street
Arlington, VA 22217-5660

10. SPONSOR/MONITOR'S ACRONYM(S)
ONR

11. SPONSORING/MONITORING AGENCY REPORT NUMBER

12. DISTRIBUTION AVAILABILITY STATEMENT
Approved for Public Release; distribution is Unlimited.

13. SUPPLEMENTARY NOTES

14. ABSTRACT

Three methods have been developed for assessing the stability of dc-to dc converters and converter-based power systems. The first of these methods is based on a state-space representation of an average-value model of a dc-to-dc buck converter with an LC input filter. It is shown that filter-converter combination is completely controllable through state feedback. The second method is based on an exact expression for the input impedance of the buck converter. This expression may be used in conjunction with the Nyquist criterion applied to the minor loop at the interface between the converter and a power system; it is valid at all frequencies, even those above the switching frequency. The third method is based on an analysis of the Floquet multipliers for the periodic solution to a general class of piecewise-linear systems operated with a switching surface that includes state and input variables as well as time. Software for computing the Floquet multipliers given an arbitrary state-space model of the piece-wise linear system and switching surface has been developed. It has been used to show regions of instability for the dc-to-dc buck converter.

15. SUBJECT TERMS
DC-to-DC converters; Power System Stability

16. SECURITY CLASSIFICATION OF:			17. LIMITATION OF ABSTRACT	18. NUMBER OF PAGES	19a. NAME OF RESPONSIBLE PERSON
a. REPORT	b. ABSTRACT	c. THIS PAGE			Jeffrey Mayer
U	U	U	UU		19b. TELEPONE NUMBER *(Include area code)* (814) 865-0242

Standard Form 298 (Rev. 8-98)
Prescribed by ANSI-Std Z39-18

MODELING AND CONTROL OF THE ARCP
IN POWER AND DRIVE SYSTEMS

Final Technical Report

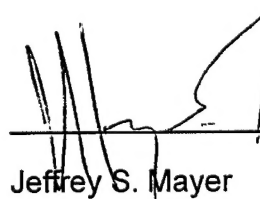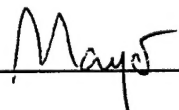Issued February 2004

for

Terry Ericsen
Office of Naval Research
Ship Structures and Systems Division
800 North Quincy Street
Arlington, VA 22217-5660

by

Jeffrey Mayer and Heath Hofmann
Department of Electrical Engineering
The Pennsylvania State University
121 EE East
University Park, PA 16802
(814) 865-0242
mayer@ee.psu.edu

Jeffrey S. Mayer   Date

OBJECTIVE

The objective of this project was to develop new models and analysis techniques for ARCP-based motor drive and power distribution systems. This was originally to include both mathematical models and experimental hardware in the form of an ARCP inverter for a quiet electric drive system and a low-power test bed representing an ARCP-based power distribution system.

APPROACH

The original approach to modeling and analyzing ARCP-based systems involved three separate tasks, one of which was mathematical and the other two experimental. The first task was to develop a behavioral model for the ARCP to be used in system studies. The second task was to develop a prototype ARCP inverter for a quiet electric drive system, and third task was to develop a low-power test bed representing an ARCP-based power distribution system. Based on a change in direction at NSWC, however, the first task was broadened to consider the analysis of systems with power converters other than the ARCP and the second task was dropped completely.

STABILITY ANALYSIS OF POWER CONVERTER SYSTEMS

The design and operation of power systems comprised of multiple power converters is challenging due to the potentially complicated dynamics in such systems. More specifically, switching is an inherently non-linear process, so common analysis and design techniques based on linear system theory cannot be applied directly. Consequently, circuit-level simulation and approximation techniques for linearizing converter models are the most widely used approaches for studying these systems. Each approach has serious drawbacks, however, and the approaches are not completely complimentary. A circuit simulation typically provides detailed information about an operating point given detailed information about a system, but owing to uncertainty in parameter values, many simulations may have to be performed and reviewed at great cost. Approximation techniques that yield a linear system model permit the use of linear system theory but may require that considerable "margin" be included in a design to accommodate the inherent discrepancies between the linear model and actual system. Moreover, approximation techniques often require considerable expertise or effort, limiting their utility.

Three new methods for analyzing the stability and/or controllability of the dc-to-dc converter systems were developed in this project. The most important aspects of each of the methods is summarized in the following subsections.

2

Stability Analysis of dc-to-dc Converter with Input Filters

The first of the new methods developed in this project centers on state-space analysis of dc-to-dc buck converters with *LC* input filters. Details of this method are described in Appendix A. The key results are: (1) a linearized state-space model of the filter/converter system is derived through average-value modeling of the switching elements, (2) the state-space model is shown to be fully controllable through complete state feedback, and (3) experiments confirm that control based on complete state feedback renders a stable system while control based only on output feedback renders an unstable system. These results should be useful to the designers of individual buck converters.

Exact Expression for Input Impedance of Buck Converters

The second of the new methods developed in this project involves the derivation of an exact expression for the input impedance of buck converters. Details of this method are described in Appendix B. The key results are: (1) an exact expression for the impedance at all frequencies and (2) a three-way comparison of the exact impedance with the approximate impedance obtained using conventional state-space averaging and the equivalent impedance obtained through detailed simulation. In general, the input impedance is useful in applying Nyquist criterion to the minor loop established when interconnecting a (load) converter to a (source) converter or distribution system. The exact impedance is valid at all frequencies above and below the switching frequency of the converter, whereas the approximate impedance derived using state-space averaging is only valid at frequencies well below the switching frequency. Thus, the new result is valuable in systems wherein converters with various switching frequencies are present, as is anticipated for shipboard systems.

Stability of Periodic Solutions for Piecewise-Linear Systems

The third of the new methods developed in this project involves the derivation of a technique for assessing the stability of the periodic solution to a wide class of systems that includes dc-to-dc converters operating in both continuous and discontinuous conduction modes. Details of this method are described in Appendix C. The key results are: (1) the derivation of the so-called monodromy matrix for piecewise-linear systems operated with a switching surface defined in terms of states, inputs, and time and (2)

3

simulations demonstrating that eigenvalue analysis of the monodromy matrix (i.e., computation of the Floquet multipliers) yields an indication of the stability of a periodic solution. The monodromy matrix derived here is for quite a general class of systems that includes as particular cases most of the dc-to-dc converters for which studies of periodic stability have been reported in the literature. A MATLAB m-file that encapsulates the highly mathematical technique has been developed to simplify its application.

DEVELOPMENT OF POWER SYSTEM STABILITY EXPERIMENTAL TESTBED

The overarching goal of this project was to investigate instabilities in power systems with power electronic components. One thrust towards this goal was the development of an experimental lab setup that would allow the investigation of power system instabilities. The results of this thrust will be described here.

Acquisition of Existing Equipment.

A significant amount of power electronic equipment was acquired from the Navy. This equipment includes:

- 51 magnetically latched electrical contactors,
- 1 phase-controlled rectifier,
- 2 9kW DC-DC "source" converters,
- a VXI mainframe with analog/digital converter and digital input/output cards,
- 12 single-pole Auxiliary Resonant Commutating Pole Inverters (hereafter referred to as ARCP's), and
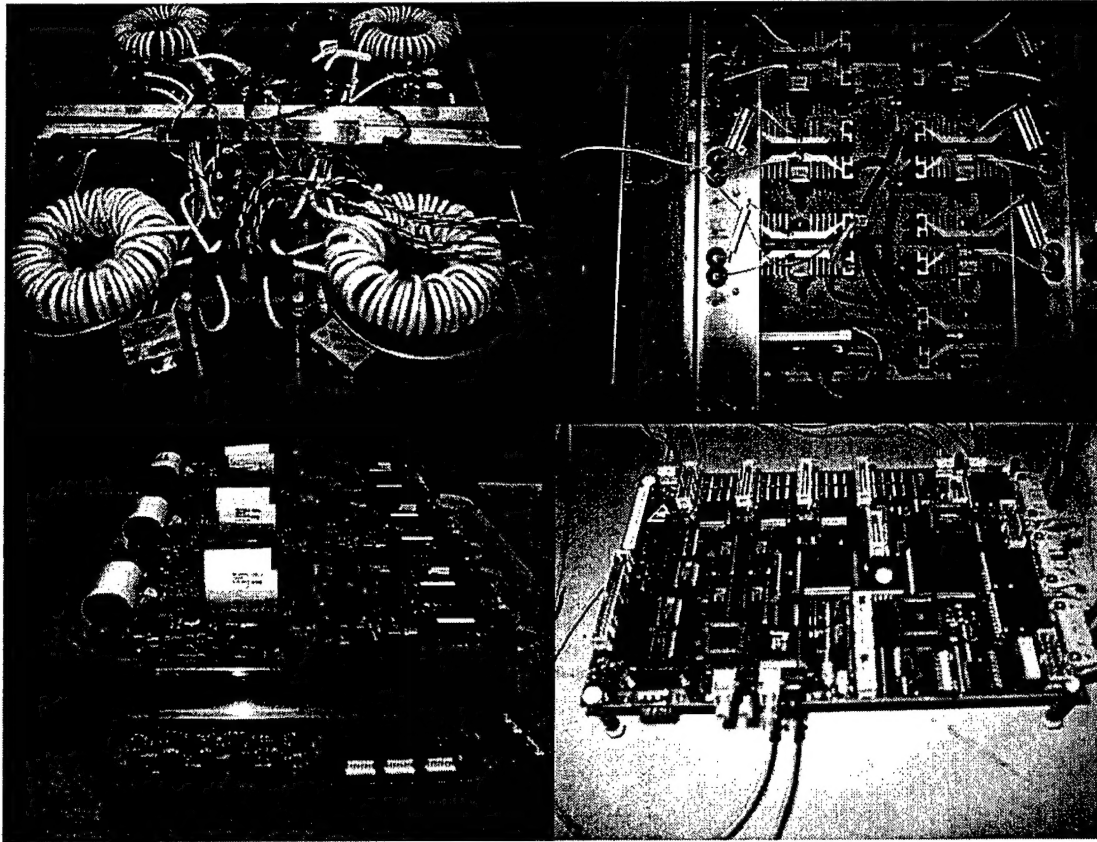- one Northrup Grumman microcontroller board.

Figure 1 Clockwise from top left: DC-DC converters, Phase-Controlled Rectifier, Northrup Grumman Controller, and ARCP inverters with sensing circuitry

Purchasing of Equipment.

The following equipment was purchased to establish the testbed.

- a Sorensen 600V, 33A DC power supply to be used in testing the existing DC-DC converters and ARCP's,
- a personal computer (PC) to act as monitoring station, controller developer, and web server for the NetSim,
- a dSPACE 1103 Controller Card. The DS1103 controller board utilizes a IBM PowerPC 604e processor running at 400 MHz, and a slave DSP, Texas Instruments' DSP TMS320F240, with which Pulse-Width-Modulated (PWM) signals are generated. The control card contains ample analog-to-digital (A/D), digital-to-analog (D/A), and digital input-output (I/O) for interfacing with the power electronic equipment.
- an anti-aliasing filter card for the VXI mainframe. This card will be used to filter analog signals representing the voltages and currents.
- a 3hp, 230V, 1800rpm induction machine, and
- a 4.5N•m, 6000rpm AC brushless permanent magnet machine.

Figure 2 Clockwise from top left: PC monitoring station w/ VXI mainframe, AC brushless PM machine, 3hp induction machine, Sorensen DC power supply

Design and Construction of Contactor Layout

Significant modifications have been made to the layout of the power system simulator. In the original design the electrical contactors were mounted on the side of a rack. In the new design the contactor layout has been reconfigured so that it may be installed inside a rack, creating a neater, more compact package as shown in Fig. 5. In addition, the electrical wiring of the contactors has been redesigned to allow a more general flexibility in the reconfiguration of the power system.

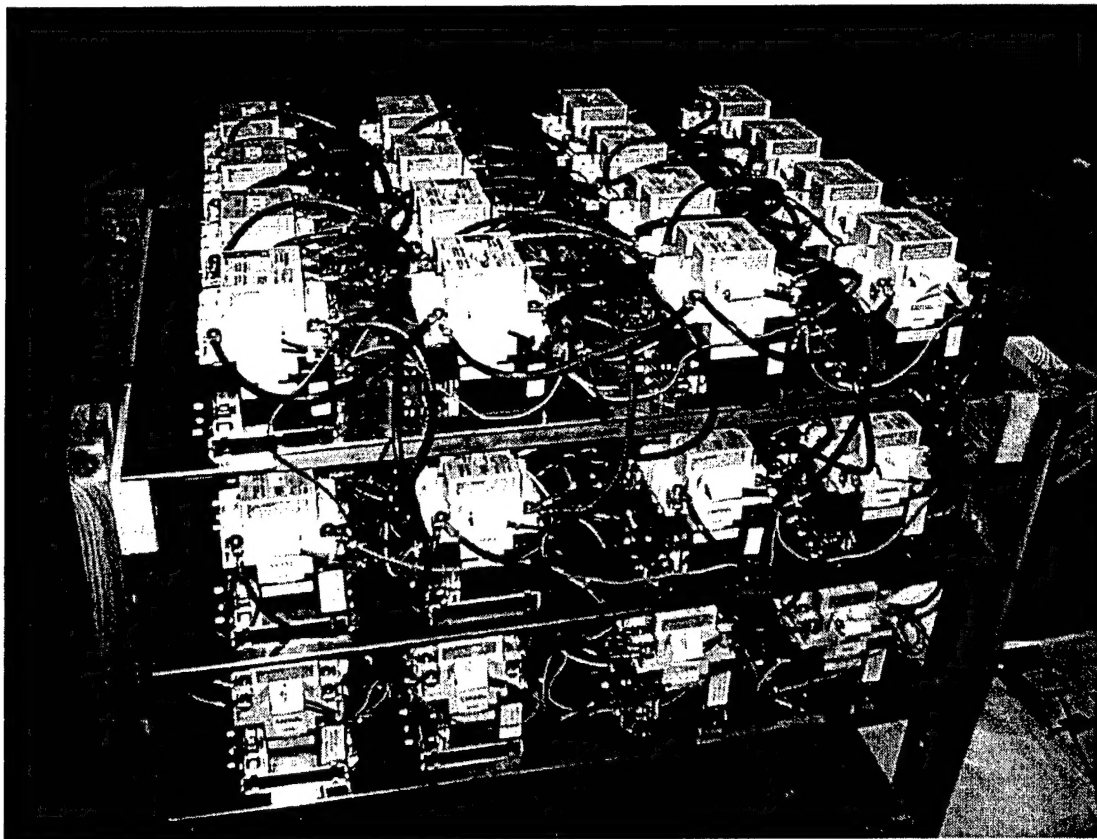Figure 3. New Electrical Contactor Configuration for NetSim

High-Performance Controller Board

Due to difficulties encountered with the acquired Northrup-Grumman controller, a high-performance controller board was designed at Penn State. The architecture of this controller consists of a floating point processor, the TI TMS320C6711, and a microcontroller, the Motorola DSP56F803. The two processors communicate via dual-

port RAM, a Cypress CY7C024AV, as will be described in a later section. The DSP chip is physically located on an evaluation board offered by Texas Instruments, shown in the following figure.
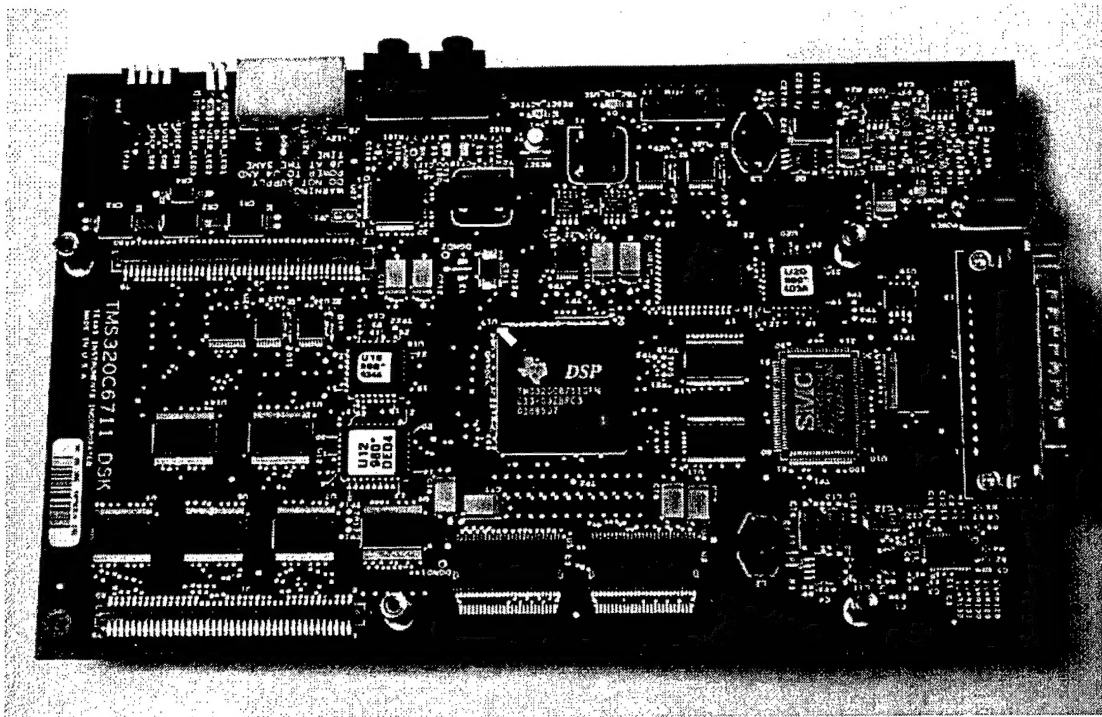
Figure 4 TI TMS320C6711 Evaluation Board

The dual-port RAM and microcontroller are located on a board designed and populated at Penn State, shown in the following figure:

Figure 5 Microcontroller Board Designed at Penn State

The Pulse-Width-Modulation outputs of the microcontroller have a fiber-optic interface, to simplify isolation requirements. The board has a JTAG interface, a potentiometer, switches, buttons, and LEDs used for testing.

In addition, a second board was designed and assembled which contains extra features, such as RAM and high-precision A/D converters. This board is shown below.

Figure 6 Board Designed at Penn State Containing RAM, High-Precision A/D Converters
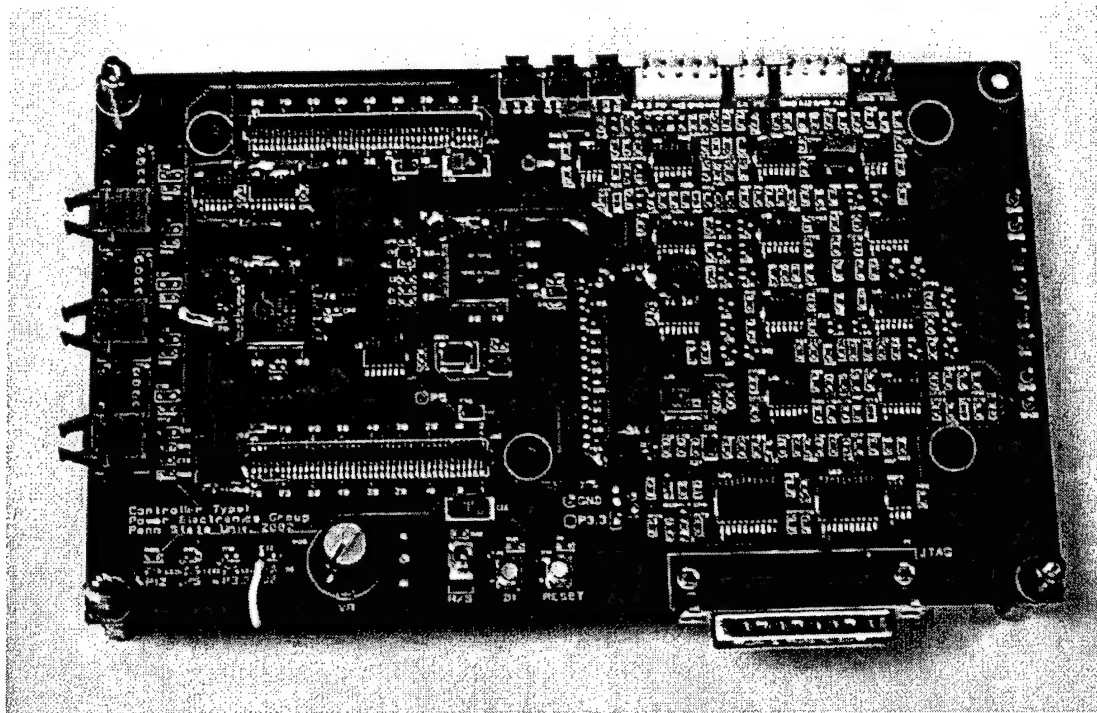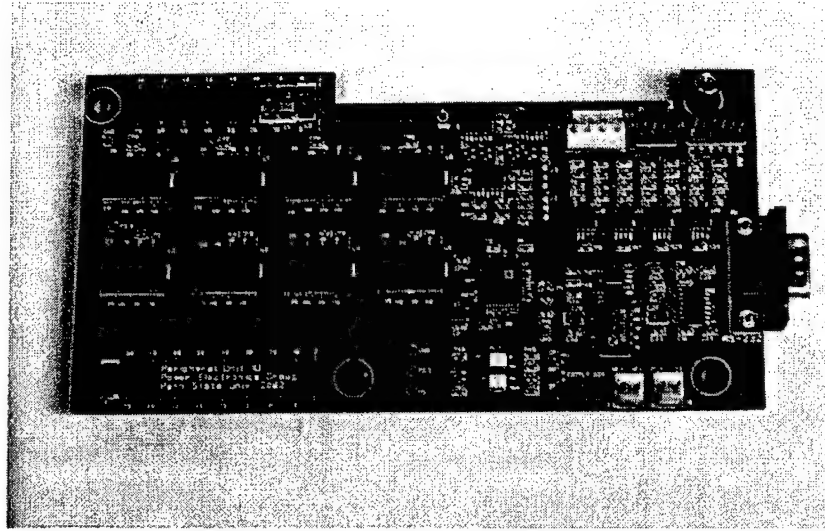
The assembled controller board configuration is shown below:
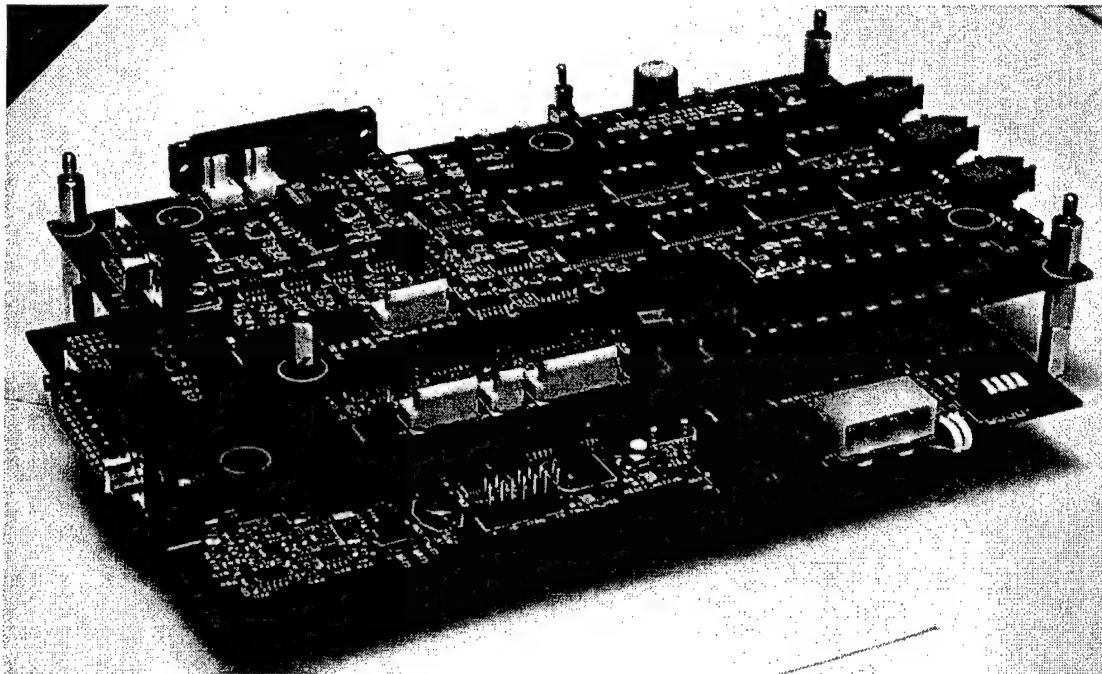

Figure 7 Assembled Controller Board

Interface Using Dual-Port Ram

Asynchronous interface between two processors using dual-port RAM offers fast, reliable and easy implementation. Even though care should be taken to design the arbitration

between processors, due to the features of today's dual-port RAM such as handling of simultaneous access of the same address and generation of some signals for communication between the ports, it has become an easier task.

The figure below shows the interface configuration between the two controller boards which have TMS320C6711 of Texas Instruments and DSP56F803 of Motorola respectively. Cypress's dual-port RAM CY7C024AV is selected for the interfacing device, which has 16-bit 1k-word, a few arbitration signals, and relatively fast access speed.
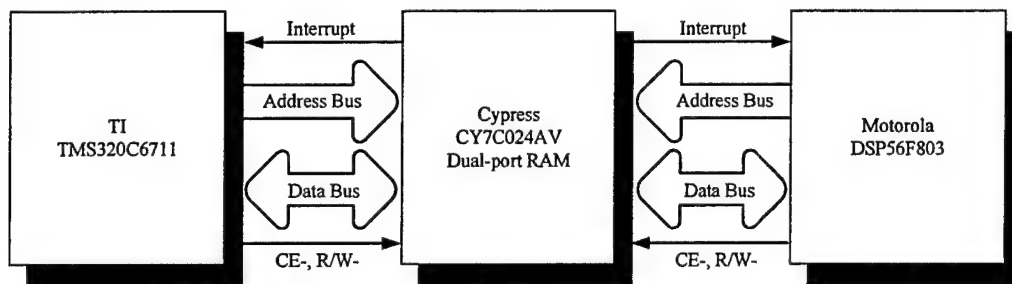

Figure 8 System Configuration

Communication Speed Test

The following communication speed test consists of sending 14 words between the two processors: eight words to the C6711, and six words to the F803. The code is written in C language for this data exchange test. The figure below represents the sequence of the code to examine communication time for 14 words..
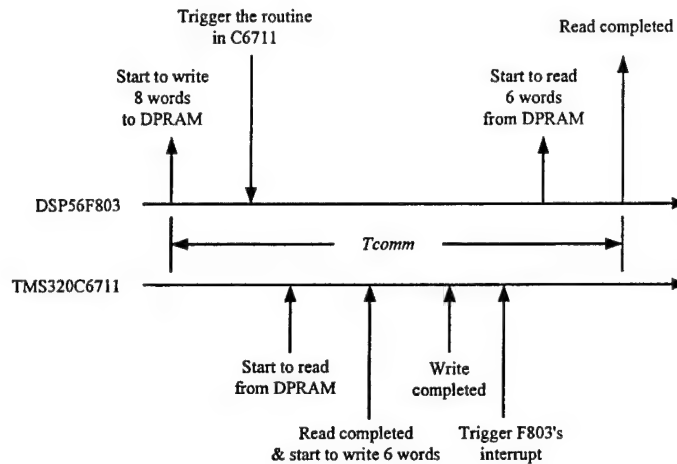
Figure 9 Sequence Diagram for Communication Test

Two modes are implemented and tested for triggering the routine in C6711 from F803, one is the "Polling mode" and another is "Interrupt mode". For the former, the C6711 "polls" a certain address of the dual-port RAM to see if the flag to start the fetching is set. This is one of the simplest implementations and if there is just one routine to run for every period and if the processor could be dedicated to poll the address during the idle time, it is possible to make it quite fast with a simple structure. But because C6711 repeatedly accesses a certain memory address with a very short period, this can reduce the dual-port RAM's lifetime and increase the possibility of failure.

The latter, triggering the C6711's routine by interrupt, can be an optimal method, because the routine is called right after the triggering. This can be easily implemented by using the interrupt generation feature in the CY7C024. But context saving and restore for the interrupt takes some time, and it might not be quite shorter than the polling period.

The communication time, T_{comm}, is determined by measuring the time between toggling of the LED on the F803 controller board. The F803 toggles the LED right before starting to write 8 words to DPRAM and after writing data, calls the routine of C6711 by writing a data to the polled address (polling mode), or to the mailbox of the dual-port RAM (interrupt mode).

If it is in the polling mode, C6711 polls a specific address every loop. Right after C6711 senses the data change, it reads the 8 words of data written by F803 from the dual-port RAM, and then writes 6 words to it. After that, the C6711 triggers the external

interrupt of F803 by writing on the mailbox in the dual-port RAM and clears the polling address.

For interrupt mode, C6711's interrupt service routine (ISR) is called by the external interrupt from dual-port RAM. This ISR has same codes with those in the main loop of polling mode. Similarly, the F803's ISR is triggered in this mode.

In the ISR in F803 for the external interrupt from dual-port RAM, F803 reads the 6 words from the dual-port RAM and toggles the LED. The time between these two LED toggling is T_{comm}, and it represents the time for feedback and commands. C codes for this speed test are listed in section IV.

Test Results

Figure 3 shows the communication speed test results. It represents the time for 14 words data exchange in polling mode (figure 3a) and interrupt mode (figure 3b). The channel 1 in the figures is the anode voltage of the LED in the DSP56F803 controller board.   It takes around 4.5 µs for both modes and does not show much difference. However, as mentioned earlier, interrupt mode will be better way for the interface design.
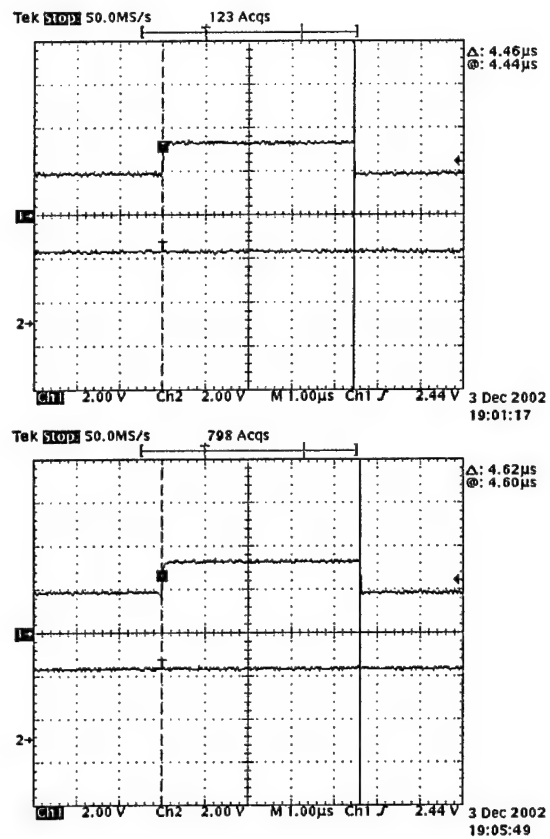
Figure 10 Communication Time Experiment. Top Figure: Polling Method. Bottom Figure: Interrupt
Method.

CONCLUSIONS AND ON-GOING WORK

Three new methods for studying the stability/controllability of dc-to-dc converter systems have been developed. The most general of these permits the rapid calculation of Floquet multipliers to assess the stability of the periodic solution to piecewise linear systems. Presently this method is being applied to self-oscillating circuits in addition to dc-to-dc converters. A future application is in an automated design environment, wherein the method would be used to assess candidate designs produced by an optimization algorithm.

APPENDIX A

Stability Analysis of DC-DC Converter Control w/ Input Filters

Abstract

This section will investigate the active stabilization of DC-DC converters with input LC filters using linear system state-space control techniques. A general continuous-time state-space-averaged model of DC-DC converter systems, including dynamics associated with the input LC filter, is presented. As an example, a buck converter with input LC filter is examined in detail. For the case of the buck converter, the linearized system is shown to be completely controllable by the duty cycle of the switching element, suggesting that feedback control of all four states (input and output capacitor voltages and inductor currents) will allow stabilizing controllers with input LC filters of arbitrary design. Experimental results confirm that regulating the states of the LC filter can stabilize the buck converter dynamics.

1 Introduction

It is well-known that the addition of an input LC filter to a DC-DC converter can create instability. The predominant technique used to study the stability of these systems has been through the use of impedance arguments based on the Nyquist criterion, as first posed by Middlebrook [1]. Using these arguments, it has been determined that feedback control of a converter is responsible for instability, as it causes the converter to present a "negative" input impedance to the system. Techniques used to resolve this problem have centered around the design of input filters that avoid this instability [2][3][4][5][6][7].

Another approach to investigate the stability of these systems is through the use of state-space techniques[8][13][9][10][11][12]. However, the use of state-space control methods to stabilize these systems up to now has not been thoroughly investigated. In this paper we will use a state-space approach to investigate the active stabilization of DC-DC converters with an arbitrarily-designed LC filter, shown in Fig. 1, through appropriate duty cycle control. We will begin by presenting the state-space averaged model that will be used for the analysis. For the purpose of this report one example, a buck converter, is investigated in detail.
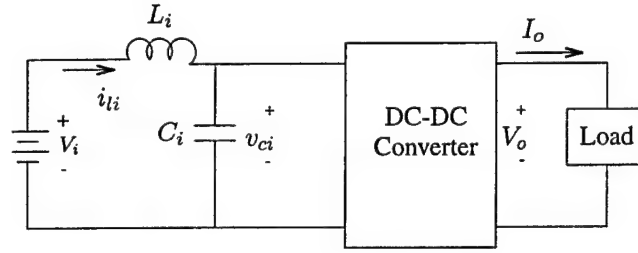
1

Figure 1: DC-DC converter system with input LC filter

2 Theoretical Background

A continuous-time model will be used for investigating stability, based upon the state-space averaging technique[13], and is briefly presented in this section. Basic DC-DC converter topologies contain a single switching "element", typically consisting of a transistor and diode, which creates a discrete change in the dynamics of the overall system based upon a duty cycle D. Assuming linear passive circuit elements (capacitors, inductors, and resistors) and neglecting the possibility of discontinuous conduction operation, the dynamics can be written in the following state-space form:

$$
\dot{\mathbf{x}} = \begin{cases} \mathbf{A}_1 \mathbf{x} + \mathbf{B}_1 \mathbf{u}, & t_k < t < t_k + DT_s, \\ \mathbf{A}_2 \mathbf{x} + \mathbf{B}_2 \mathbf{u}, & t_k + DT_s < t < t_{k+1}, \end{cases} \tag{1}
$$

where $\mathbf{x}$ is the state of the energy-storing elements in the converter, $\mathbf{u}$ represents the DC sources and loads of the converter, T_s is the switching period of the switching element, and D is the duty cycle, which is assumed in the following analysis to be a continuous variable. The average-value of the system state is given by

$$
\bar{\mathbf{x}}(t) = \int_{t-T}^{t} \mathbf{x}(s)ds, \tag{2}
$$

Under the assumption of small ripple conditions (i.e., the switching harmonics do not have a significant effect on the average-value dynamics), the average-value dynamics can be approximated as:

$$
\dot{\bar{\mathbf{x}}} \approx [D\mathbf{A}_1 + (1-D)\mathbf{A}_2]\bar{\mathbf{x}} + [D\mathbf{B}_1 + (1-D)\mathbf{B}_2]\mathbf{u} \tag{3}
$$

In this case the switching element is replaced by controlled sources, as shown in Fig. 2. The average-value state error $\bar{\mathbf{e}}$ is defined by

$$
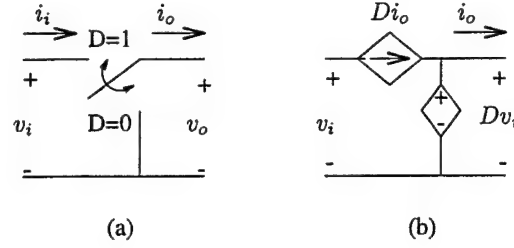\bar{\mathbf{e}} = \bar{\mathbf{x}} - \tilde{\mathbf{x}}, \tag{4}
$$

Figure 2: Switching element and equivalent model under the state-space averaging technique

, where $\bar{\mathbf{x}}$ is the desired DC state of the overall system. For this presentation we choose the duty cycle D to contain a feedforward term $\tilde{D}$, which would in theory achieve the desired state $\bar{\mathbf{x}}$, and a feedback term $g(\mathbf{e})$

$$D = \tilde{D} + g(\mathbf{e}) \tag{5}$$

Under these conditions, the average-value error dynamics can be shown to be:

$$\dot{\bar{\mathbf{e}}} = \left[\tilde{D}\mathbf{A}_1 + \left(1 - \tilde{D}\right)\mathbf{A}_2\right]\bar{\mathbf{e}} + [(\mathbf{A}_1 - \mathbf{A}_2)\bar{\mathbf{x}} + (\mathbf{B}_1 - \mathbf{B}_2)\mathbf{u}]\,g(\bar{\mathbf{e}}) + (\mathbf{A}_1 - \mathbf{A}_2)\bar{\mathbf{e}}g(\bar{\mathbf{e}})$$

$$= \mathbf{A}_e\bar{\mathbf{e}} + \mathbf{b}_e g(\bar{\mathbf{e}}) + h.o.t. \tag{6}$$

Due to the DC nature of the operating point of the converter, it is convenient and appropriate to neglect the higher-order error terms. Using this form, linear system theory can be used to determine appropriate methods of stabilizing the controller while achieving sufficient closed-loop bandwidth. The feedback term can consist of PID or any other type of feedback control. For the purposes of this paper we will concentrate on proportional feedback control of (potentially) all states of the system:

$$D = \tilde{D} + \mathbf{k}^T\mathbf{e} \qquad . \tag{7}$$

Although this type of control may be insufficient for a practical system, it will serve to make fundamental conclusions regarding the active stabilization of the overall system. It should also be noted that our converter models neglects loss mechanisms, which can also have a significant effect on the stability of the system. Once again, our goal is to make fundamental conclusions regarding stability rather than generate precise results.

3 Example: Buck converter with input LC filter

We will study the control of the DC-DC "buck" converter design shown in Figure 3. Parameters for the converter, which will be
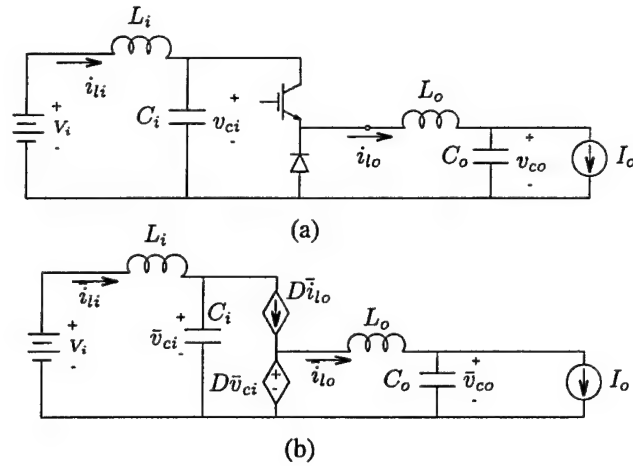
Figure 3: DC-DC "buck" converter with input LC filter. Top figure: actual circuit. Bottom figure: equivalent "average-value" model

Input Inductance (L_i)	$100mH$
Input Capacitance (C_i)	$1mF$
Output Inductance (L_o)	$10mH$
Output Capacitance (C_o)	$470\mu F$
Input Voltage (V_i)	$24V$
Output Voltage (V_o)	$12V$
Output Current (I_o)	$6A$

Table 1: Component and Operating Point Parameters of Example DC-DC "Buck" Converter

used in the stability analysis, are provided in Table 1:

We will assume that we desire an output voltage $\tilde{V}_o$ and that we are measuring the output current I_o, which is assumed constant. We will also command an "input" voltage $v_{ci} = V_i$ and an input current $i_{li} = \frac{\tilde{V}_o}{V_i} I_o$. Using the state-space averaging technique and assuming continuous current conduction, the dynamics of the average-value system variables are given by the following set of equations:

$$\dot{v}_{ci} = \frac{1}{C_i}(i_{li} - Di_{lo})$$

$$\dot{i}_{li} = \frac{1}{L_i}(V_i - v_{ci})$$

$$\dot{v}_{co} = \frac{1}{C_o}(i_{lo} - I_o)$$

$$\dot{i}_{lo} = \frac{1}{L_o}(Dv_{ci} - v_{co}) \tag{8}$$

or

$$\frac{d}{dt}\begin{bmatrix} v_{ci} \\ i_{li} \\ v_{co} \\ i_{lo} \end{bmatrix} = \begin{bmatrix} 0 & \frac{1}{C_i} & 0 & -\frac{D}{C_i} \\ -\frac{1}{L_i} & 0 & 0 & 0 \\ 0 & 0 & 0 & \frac{1}{C_o} \\ \frac{D}{L_o} & 0 & -\frac{1}{L_o} & 0 \end{bmatrix}\begin{bmatrix} v_{ci} \\ i_{li} \\ v_{co} \\ i_{lo} \end{bmatrix} + \begin{bmatrix} 0 & 0 \\ \frac{1}{L_i} & 0 \\ 0 & -\frac{1}{C_o} \\ 0 & 0 \end{bmatrix}\begin{bmatrix} V_i \\ I_o \end{bmatrix} \tag{9}$$

We define the following error terms:

$$e_{ci} = v_{ci} - V_i$$

$$e_{li} = i_{li} - \frac{\tilde{V}_o}{V_i}I_o$$

$$e_{co} = v_{co} - \tilde{V}_o$$

$$e_{lo} = i_{lo} - I_o \tag{10}$$

Using these terms, the error dynamics can be written as follows:

$$\frac{d}{dt}\begin{bmatrix} e_{ci} \\ e_{li} \\ e_{co} \\ e_{lo} \end{bmatrix} = \begin{bmatrix} 0 & \frac{1}{C_i} & 0 & -\frac{D}{C_i} \\ -\frac{1}{L_i} & 0 & 0 & 0 \\ 0 & 0 & 0 & \frac{1}{C_o} \\ \frac{D}{L_o} & 0 & -\frac{1}{L_o} & 0 \end{bmatrix}\begin{bmatrix} e_{ci} \\ e_{li} \\ e_{co} \\ e_{lo} \end{bmatrix} + \begin{bmatrix} 0 & 0 & \frac{1}{C_i}\left(\frac{\tilde{V}_o}{V_i} - D\right) \\ 0 & 0 & 0 \\ 0 & 0 & 0 \\ -\frac{1}{L_o} & \frac{D}{L_o} & 0 \end{bmatrix}\begin{bmatrix} \tilde{V}_o \\ V_i \\ I_o \end{bmatrix} \tag{11}$$

We choose the following duty cycle for control:

$$D = \frac{\tilde{V}_o}{V_i} + \frac{1}{V_i}(K_{ci}e_{ci} + K_{li}e_{li} + K_{co}e_{co} + K_{lo}e_{lo})$$

$$= \tilde{D} + \frac{1}{V_i}u(t) \tag{12}$$

The dynamics now become:

$$\frac{d}{dt}\begin{bmatrix} e_{ci} \\ e_{li} \\ e_{co} \\ e_{lo} \end{bmatrix} = \begin{bmatrix} 0 & \frac{1}{C_i} & 0 & -\frac{\tilde{D}}{C_i} \\ -\frac{1}{L_i} & 0 & 0 & 0 \\ 0 & 0 & 0 & \frac{1}{C_o} \\ \frac{\tilde{D}}{L_o} & 0 & -\frac{1}{L_o} & 0 \end{bmatrix}\begin{bmatrix} e_{ci} \\ e_{li} \\ e_{co} \\ e_{lo} \end{bmatrix} + \begin{bmatrix} -\frac{I_o}{V_iC_i} \\ 0 \\ 0 \\ \frac{1}{L_o} \end{bmatrix}u + h.o.t. \tag{13}$$

We define:

$$
\mathbf{A}_e \;=\; \begin{bmatrix} 0 & \frac{1}{C_i} & 0 & -\frac{\tilde{D}}{C_i} \\[2mm] -\frac{1}{L_i} & 0 & 0 & 0 \\[2mm] 0 & 0 & 0 & \frac{1}{C_o} \\[2mm] \frac{\tilde{D}}{L_o} & 0 & -\frac{1}{L_o} & 0 \end{bmatrix}
$$

$$
\mathbf{b}_e \;=\; \begin{bmatrix} -\frac{I_o}{V_i C_i} \\[2mm] 0 \\[2mm] 0 \\[2mm] \frac{1}{L_o} \end{bmatrix}
$$

$$
\mathbf{k}^T \;=\; \begin{bmatrix} K_{ci} & K_{li} & K_{co} & K_{lo} \end{bmatrix}
$$

We can analyze this system of equations using standard linear control theory by neglecting the higher-order terms and focusing on small-signal controllability and stability. Our first step is to check controllability; if controllable, we then attempt to determine values of K_{ci}, K_{li}, K_{co} and K_{lo} that will allow us to achieve stability.

3.1 Controllability

The controllability matrix [14] of the above linearized system,

$$
\mathbf{M} \;=\; \begin{bmatrix} \mathbf{b}_e & \mathbf{A}_e\mathbf{b}_e & \mathbf{A}_e^2\mathbf{b}_e & \mathbf{A}_e^3\mathbf{b}_e \end{bmatrix} \tag{14}
$$

can be shown to have the following determinant:

$$
|\mathbf{M}| \;=\; \frac{\tilde{D}^2 L_i C_o \left[L_o I_o^2 + C_i V_i^2 \right]\left[L_i I_o^2 + C_o V_i^2 \right] + I_o^2 \left(C_o L_o - C_i L_i \right)^2}{C_i^4 L_i^3 C_o^3 L_o^4} \tag{15}
$$

Inspection of (15) reveals that it is positive regardless of circuit parameters and loading conditions, hence the controllability matrix will always have full rank and the overall system is controllable. Therefore, in theory the poles of the system can be arbitrarily placed and therefore an arbitrary bandwidth can be prescribed to the controller if all four states of the system (input and output inductor currents and capacitor voltages) are regulated. In practice bandwidths will be limited by the switching frequency of the converter. The main contribution of the above analysis is the notion that incorporating feedback of the input filter inductor current and/or capacitor voltage into the duty cycle of the converter can stabilize the overall system, regardless of the input LC filter design.

3.2 Stability Analysis

3.2.1 Stability Analysis of Output State Control Only

We first analyze the stability of the system when only the output states of the converter are regulated (i.e., $K_{ci} = K_{li} = 0$). The characteristic equation of the system is:

$$
\begin{aligned}
\left| \mathbf{A}_e + \mathbf{b}_e \mathbf{k}^T - \lambda \mathbf{I} \right| =\ & \lambda^4 + \frac{I_o \lambda^3 K_{ci}}{C_i V_i} - \frac{K_{lo} \lambda^3}{L_o} + \frac{\lambda^2}{C_i L_i} + \frac{D^2 \lambda^2}{C_i L_o} + \frac{\lambda^2}{C_o L_o} - \frac{K_{co} \lambda^2}{C_o L_o} \\
& - \frac{I_o K_{li} \lambda^2}{C_i L_i V_i} + \frac{I_o D K_{lo} \lambda^2}{C_i V_i L_o} + \frac{D K_{ci} \lambda^2}{C_i L_o} + \frac{I_o K_{ci} \lambda}{C_i C_o L_o V_i} - \frac{D K_{li} \lambda}{C_i L_i L_o} - \frac{K_{lo} \lambda}{C_i L_i L_o} \\
& + \frac{I_o D K_{co} \lambda}{C_i C_o L_o V_i} + \frac{1}{C_i L_i C_o L_o} - \frac{K_{co}}{C_i L_i C_o L_o} - \frac{I_o K_{li}}{C_i L_i C_o L_o V_i} \\
=\ & 0
\end{aligned}
\tag{16}
$$

or:

$$
\left(\lambda^4 + \frac{\lambda^2}{C_i L_i} + \frac{D^2 \lambda^2}{C_i L_o} + \frac{\lambda^2}{C_o L_o} + \frac{1}{C_i L_i C_o L_o} \right) + \begin{bmatrix} K_{ci} & K_{li} & K_{co} & K_{lo} \end{bmatrix} \begin{bmatrix} \frac{\lambda^3 I_o}{C_i V_i} + \frac{D \lambda^2}{C_i L_o} + \frac{I_o \lambda}{C_i C_o L_o V_i} \\[4pt] -\frac{I_o \lambda^2}{C_i L_i V_i} - \frac{D \lambda}{C_i L_i L_o} - \frac{I_o}{C_i L_i C_o L_o V_i} \\[4pt] -\frac{\lambda^2}{C_o L_o} + \frac{I_o D \lambda}{C_i C_o L_o V_i} - \frac{1}{C_i L_i C_o L_o} \\[4pt] -\frac{\lambda^3}{L_o} + \frac{I_o D \lambda^2}{C_i V_i L_o} - \frac{\lambda}{C_i L_i L_o} \end{bmatrix} = 0 \tag{17}
$$

In order to determine the marginal stability condition, i.e., when at least two of the four eigenvalues of $\mathbf{A}_e + \mathbf{b}_e \mathbf{k}^T$ are on the imaginary axis(or one of the four is zero), we set $\lambda = j\omega$, and substitute it into eq. (17), and set $K_{ci}, K_{li} = 0$. The result is:

$$
\begin{aligned}
\left(\omega^4 - \frac{\omega^2}{C_i L_i} - \frac{D^2 \omega^2}{C_i L_o} - \frac{\omega^2}{C_o L_o} + \frac{1}{C_i L_i C_o L_o} \right) + K_{co} \left(\frac{\omega^2}{C_o L_o} + \frac{I_o D j \omega}{C_i C_o L_o V_i} - \frac{1}{C_i L_i C_o L_o} \right) & \\
+ K_{lo} \left(\frac{j \omega^3}{L_o} - \frac{I_o D \omega^2}{C_i V_i L_o} - \frac{j \omega}{C_i L_i L_o} \right) & = 0
\end{aligned}
\tag{18}
$$

If we split the real component and the imaginary component of this complex expression, the equation for real part is:

$$
\left(\frac{\omega^2}{C_o L_o} - \frac{1}{C_i L_i C_o L_o} \right) K_{co} - \frac{I_o D \omega^2}{C_i V_i L_o} K_{lo} = -\omega^4 + \frac{\omega^2}{C_i L_i} + \frac{D^2 \omega^2}{C_i L_o} + \frac{\omega^2}{C_o L_o} - \frac{1}{C_i L_i C_o L_o} \tag{19}
$$

And the imaginary component is:

$$
\frac{I_o D \omega}{C_i C_o L_o V_i} K_{co} + \left(\frac{\omega^3}{L_o} - \frac{\omega}{C_i L_i L_o} \right) K_{lo} = 0 \tag{20}
$$

These expressions can therefore be written in matrix form:

$$
\begin{bmatrix} \frac{\omega^2}{C_o L_o} - \frac{1}{C_i L_i C_o L_o} & -\frac{I_o D \omega^2}{C_i V_i L_o} \\[6pt] \frac{I_o D \omega}{C_i C_o L_o V_i} & \frac{\omega^3}{L_o} - \frac{\omega}{C_i L_i L_o} \end{bmatrix} \begin{bmatrix} K_{co} \\[6pt] K_{lo} \end{bmatrix} = \begin{bmatrix} -\omega^4 + \frac{\omega^2}{C_i L_i} + \frac{D^2 \omega^2}{C_i L_o} + \frac{\omega^2}{C_o L_o} - \frac{1}{C_i L_i C_o L_o} \\[6pt] 0 \end{bmatrix} \tag{21}
$$

If we define:

$$\mathbf{T} = \begin{bmatrix} \frac{\omega^2}{C_o L_o} - \frac{1}{C_i L_i C_o L_o} & -\frac{I_o D \omega^2}{C_i V_i L_o} \\[2mm] \frac{I_o D \omega}{C_i C_o L_o V_i} & \frac{\omega^3}{L_o} - \frac{\omega}{C_i L_i L_o} \end{bmatrix}$$

$$\mathbf{RR} = \begin{bmatrix} -\omega^4 + \frac{\omega^2}{C_i L_i} + \frac{D^2 \omega^2}{C_i L_o} + \frac{\omega^2}{C_o L_o} - \frac{1}{C_i L_i C_o L_o} \\[2mm] 0 \end{bmatrix}$$

(22)

then

$$\begin{bmatrix} K_{co} \\[2mm] K_{lo} \end{bmatrix} = \mathbf{T}^{-1}\mathbf{RR}$$

(23)

When $\omega = 0$, $\mathbf{T}$ is singular. In this condition, it can be shown that a marginally stable system occurs when $K_{co} = 1$. With the obtained K_{co}, K_{lo}, we calculate the corresponding eigenvalues of the system and keep the points that make the system at least marginally stable. Finally we get the locus of K_{co} and K_{lo} that make the system at least marginally stable, as shown in Fig. 3.2.1. As will be shown in the next section, the interior of the locus consists of the set of K_{co} and K_{lo} combinations that make the system stable.

3.2.2 Analysis with Routh-Hurwitz Method

When $K_{ci}, K_{li} = 0$, the characteristic equation becomes:

$$\lambda^4 - \frac{K_{lo}}{L_o}\lambda^3 + \left(\frac{1}{C_i L_i} + \frac{D^2}{C_i L_o} + \frac{1}{C_o L_o} - \frac{K_{co}}{C_o L_o} + \frac{I_o D K_{lo}}{C_i V_i L_o} \right)\lambda^2$$

$$+ \left(\frac{I_o D K_{co}}{C_i C_o L_o V_i} - \frac{K_{lo}}{C_i L_i L_o} \right)\lambda + \left(\frac{1}{C_i L_i C_o L_o} - \frac{K_{co}}{C_i L_i C_o L_o} \right) = 0$$

(24)

The Routh-Hurwitz Criterion Table is therefore given by:

s^4	1	$\frac{1}{C_i L_i} + \frac{D^2}{C_i L_o} + \frac{1}{C_o L_o} - \frac{K_{co}}{C_o L_o} + \frac{I_o D K_{lo}}{C_i V_i L_o}$	$\frac{1}{C_i L_i C_o L_o} - \frac{K_{co}}{C_i L_i C_o L_o}$
s^3	$-\frac{K_{lo}}{L_o}$	$\frac{I_o D K_{co}}{C_i C_o L_o V_i} - \frac{K_{lo}}{C_i L_i L_o}$	0
s^2	$\frac{D^2}{C_i L_o} + \frac{1}{C_o L_o} - \frac{K_{co}}{C_o L_o} + \frac{I_o D K_{lo}}{C_i V_i L_o} + \frac{I_o D K_{co}}{C_i C_o V_i K_{lo}}$	$\frac{1}{C_i L_i C_o L_o} - \frac{K_{co}}{C_i L_i C_o L_o}$	
s^1	$\frac{tt}{\frac{D^2}{C_i L_o} + \frac{1}{C_o L_o} - \frac{K_{co}}{C_o L_o} + \frac{I_o D K_{lo}}{C_i V_i L_o} + \frac{I_o D K_{co}}{C_i C_o V_i K_{lo}}}$		
s^0	$\frac{1}{C_i L_i C_o L_o} - \frac{K_{co}}{C_i L_i C_o L_o}$		

where

$$tt = \left(-I_o D K_{co}^2 C_i V_i L_i K_{lo} + D^3 I_o K_{co} V_i C_o L_i K_{lo} + I_o D K_{co} C_i V_i L_i K_{lo} \right.$$

$$\left. + I_o^2 D^2 K_{co} K_{lo}^2 C_o L_i + I_o^2 D^2 K_{co}^2 L_o L_i - K_{lo}^2 D^2 V_i^2 C_o^2 - I_o D K_{lo}^3 V_i C_o^2 - I_o D K_{co} L_o V_i C_o K_{lo} \right) / \left(C_i^2 L_o^2 V_i^2 C_o^2 L_i K_{lo} \right)$$
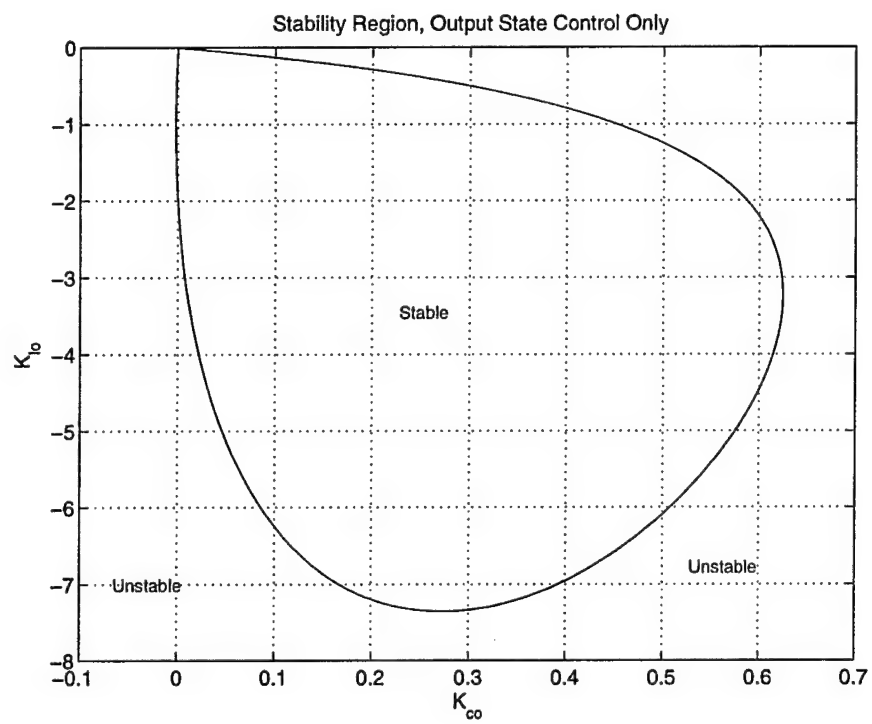
Figure 4: Locus of Marginally Stable Controller Parameters

From the table we see that a stable system must satisfy the following conditions:

$$-\frac{K_{lo}}{L_o} > 0 \tag{25}$$

$$\frac{D^2}{C_iL_o} + \frac{1}{C_oL_o} - \frac{K_{co}}{C_oL_o} + \frac{I_oDK_{lo}}{C_iV_iL_o} + \frac{I_oDK_{co}}{C_iC_oV_iK_{lo}} > 0 \tag{26}$$

$$-I_oDK_{co}^2C_iV_iL_iK_{lo} + D^3I_oK_{co}V_iC_oL_iK_{lo} + I_oDK_{co}C_iV_iL_iK_{lo}$$

$$+I_o^2D^2K_{co}K_{lo}^2C_oL_i + I_o^2D^2K_{co}^2L_oL_i - K_{lo}^2D^2V_i^2C_o^2$$

$$-I_oDK_{lo}^3V_iC_o^2 - I_oDK_{co}L_oV_iC_oK_{lo} < 0 \tag{27}$$

$$\frac{1}{C_iL_iC_oL_o} - \frac{K_{co}}{C_iL_iC_oL_o} > 0 \tag{28}$$

From eq.(25), we get

$$K_{lo} < 0 \tag{29}$$

From eq.(26), we get

$$K_{lo}D^2C_oV_i + C_iV_iK_{lo} - K_{co}C_iV_iK_{lo} + I_oDK_{lo}^2C_o + I_oDK_{co}L_o < 0 \tag{30}$$

From eq.(27), we get

$$-I_oK_{co}^2C_iL_iV_iK_{lo} + D^2I_oK_{co}K_{lo}V_iC_oL_i + I_oK_{co}C_iV_iL_iK_{lo} + I_o^2DK_{co}K_{lo}^2C_oL_i$$

$$+I_o^2DK_{co}^2L_oL_i - K_{lo}^2DV_i^2C_o^2 - I_oK_{lo}^3V_iC_o^2 - I_oK_{co}K_{lo}L_oV_iC_o < 0 \tag{31}$$

From eq.(28), we get

$$K_{co} < 1 \tag{32}$$

By testing the values of (K_{co}, K_{lo}), we find that we get the same locus as displayed in Fig. 3.2.1. Furthermore, Routh-Hurwitz explicitly shows that it is the interior of the locus that consists of the stable control parameters.

The results of this analysis show that the range of stable control parameters for this system is quite small. This is exacerbated by the fact that, in practice, we would limit the value of K_{co} to negative values, as regulation of the output voltage is usually the main priority of the controller. In this case the set of stable control parameters is essentially negligible. Another conclusion drawn from the locus is that, with output state control only, regulation of the output inductor current is essential to achieving stability.
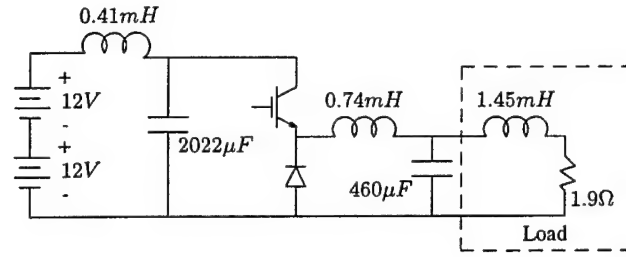
Figure 5: Buck converter system in the experiment

4 Experimental Results: Buck converter with input LC filter

To illustrate the validity of the previous analysis, experiments have been performed on the NETSIM buck converter with input LC filter. To avoid the interaction of the converter with the inner dynamics of regulated DC power supplies, batteries were used for the input voltage V_i. Control of the converter was implemented using a dSpace DS1103 controller card. The DS1103 controller board utilizes a IBM PowerPC 604e processor running at $400MHz$, and a slave DSP, Texas Instruments' DSP TMS320F240, with which PWM signals are generated. The update of the commanded duty cycle and sampling of the converter states was performed in synchronous with the switching frequency.

The experimental buck converter circuit is the NETSIM converter discussed previously. The component parameters of this converter are those of the example in the previous section. For this experiment two $12V$ batteries were series-linked as the input power supply (hence $V_i = 24V$. The commanded output voltage in the experiments was $V_o = 12V$. An RL circuit was used for the load, resulting in an output current of approximately $I_o = 6A$. The switching frequency of the IGBT in these experiments was $20kHz$. At this operating point the buck converter was operating in continuous-conduction mode. A diagram of the setup is shown in Fig. 5.

In the first experiment, only output states(v_{co} and i_{lo}) were regulated, i.e., the control gains for the input state variables were set to be zero. The output control gains were increased until an instability was generated, as can be seen in Fig. 6. In the second experiment, the control gains of the output states are the same as in the first experiment, but the input capacitor voltage is also regulated($K_{ci} = -3$). Inspection of Fig. 7 reveals that this additional regulation eliminates the instability.
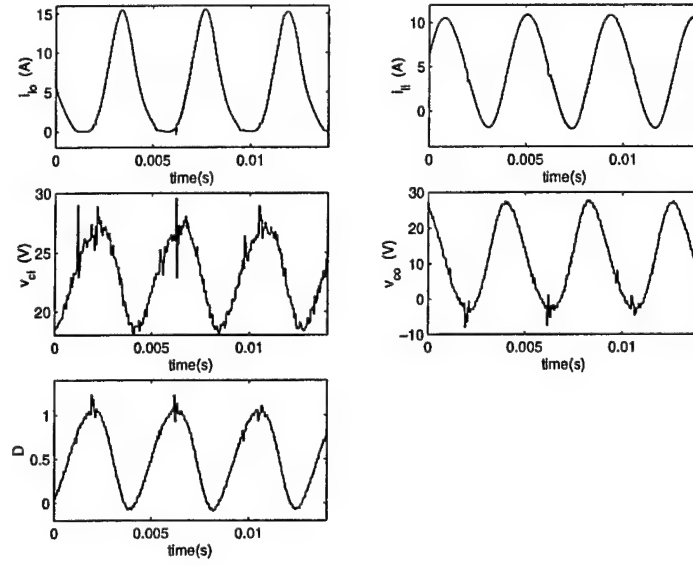
Figure 6: Unstable operation of controller w/ regulation of only output states: $K_{co} = -0.81, K_{lo} = -0.3$ and $K_{ci} = K_{li} = 0$
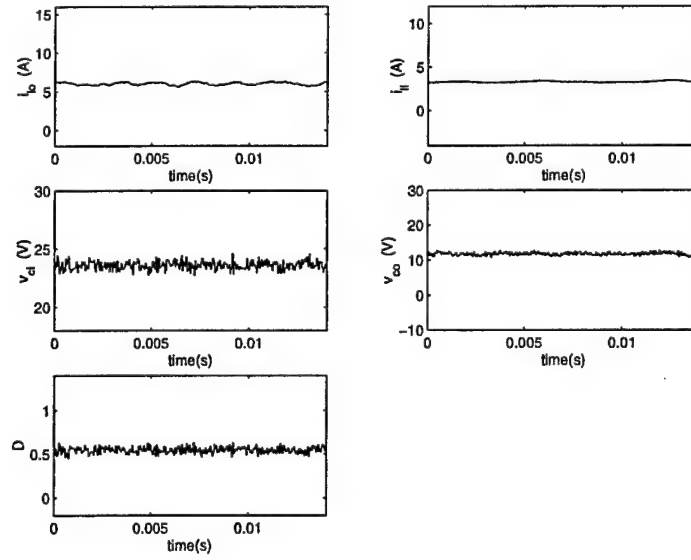
Figure 7: Stable operation of controller w/ regulation of input and output states: $K_{co} = -0.81$, $K_{lo} = -0.3$, $K_{ci} = -3$ and $K_{li} = 0$

5 Conclusion

A method of actively stabilizing DC-DC converters w/ input LC filters has been presented. A buck converter was analyzed as an example and revealed that, with addition of feedback control of the states of the input LC filter, the overall system is fully controllable, and therefore that the converter can be stabilized regardless of input filter design. Experiment results on a buck converter verifies the conclusion of the analysis.

References

[1] R.D. Middlebrook. Input filter considerations in design and application of switching regulators. *Proceedings of the IEEE Industry Applications Society Annual Meeting*, pages 91–107, Oct 1976.

[2] D.M. Mitchell. Power line filter design considerations for dc-dc converters. *IEEE Industry Applications Magazine*, 5(6):16–26, Nov.-Dec. 1999.

[3] M. Florez-Lizarraga and A. Witulski. Input filter design for multiple-module dc power systems. *IEEE Transactions on Power Electronics*, 11(3):472–479, May 1996.

[4] C.R. Kohut. Input filter design criteria for switching regulators using current-mode programming. *IEEE Transactions on Power Electronics*, 7(3):469–479, July 1992.

[5] S.Y. Erich and W.M. Polivka. Input filter design criteria for current-programmed regulators. *IEEE Transactions on Power Electronics*, 7(1):143–151, Jan. 1992.

[6] Y. Jang and R.W. Erickson. Physical origins of input filter oscillations in current programmed converters. *IEEE Transactions on Power Electronics*, 7(4):725–733, Oct. 1992.

[7] A. Emadi and M. Ehsani. Negative impedance stabilizing controls for pwm dc/dc converters using feedback linearization techniques. *Proceedings of the Intersociety Energy Conversion Engineering Conference,35th Intersociety Energy Converson Engineering Conference*, pages 613–620, July 2000.

[8] R.D. Middlebrook and S. Cuk. A general unified approach to modelling switching-converter power stages. *International Journal of Electronics*, 42(6):521–550, 1977.

[9] M. Belkhayat, R. Cooley, and E.H. Abed. Stability and dynamics of power systems with regulated converters. *IEEE International Symposium on Circuits and Systems*, 1:143–145, Apr 30-May 3 1995.

[10] A.J. Forsyth and S.V. Molloy. Modelling and control of dc-dc converters. *Power Engineering Journal*, 12(5):229–236, Oct. 1998.

[11] J. Emadi J. Mahdavi and H.A. Toliyat. Application of state space averaging method to sliding mode control of pwm dc/dc converters. *IEEE Industry Applications Society Annual Meeting*, pages 820–827, Oct. 5-9 1997.

[12] S.D. Sudhoff and S.F. Glover. Three-dimensional stability analysis of dc power electronics based systems. *Power Electronics Specialists Conference*, 1:101–106, 2000.

[13] R.D. Middlebrook and S. Cuk. Modelling and analysis methods for dc-to-dc switching converters. *Proceedings of the IEEE international semiconductor Power Converter Conference*, pages 90–111, March 1977.

[14] F.M. Callier and C.A. Desoer. *Linear System Theory*. Springer-Verlag, New York, 1991.

APPENDIX B

An Exact Expression for the Input Impedance
of the Buck Converter in Continuous Conduction Mode

S. G. Kriventsov and J. S. Mayer
Department of Electrical Engineering
The Pennsylvania State University
121 EE East
University Park, PA 16802

Abstract – A general method of exact calculation of frequency characteristics of outputs for piecewise-LTI (linear time-invariant) periodic systems with periodic inputs is developed. The method is used to find the input impedance of a switching buck converter in continuous conduction mode.

I. INTRODUCTION

Methods to ensure the stability of dc power distribution systems that are comprised of several more-or-less independently designed and operated source and load converters have received considerable attention in recent years [1-4]. Prominent among these methods is a family of criteria based on a comparison of equivalent source and load impedances, which represent the parallel aggregation of all sources and loads, respectively, in a linearized model of the system. More specifically, the ratio of the equivalent source output impedance to the equivalent load input impedance is taken as a minor loop gain that must satisfy the Nyquist stability criterion [5] to ensure the stability of the linearized system. It is assumed (usually without rigorous justification) that the results of stability analysis for the linearized system will also be valid for the actual system. Various stability criteria in this family differ in the form of a so-called forbidden region that is related to restrictions on the value of the source-to-load impedance ratio that are introduced to ensure that the Nyquist criterion is satisfied. An aspect common to all criteria, however, is the need to characterize the source and load impedances over the whole interval of frequencies for which the minor loop gain can encircle the point $-1 + j0$ in the complex plane.

Due to the switching nonlinearity of power converters, frequency characterization of their input or output impedance for stability analysis is not a trivial task. Two different approaches can be used. The first approach is based on analytical average-value modeling of the system. Since the Nyquist criterion is valid only for linear plants, a linearized model of the system is required, which is achieved by averaging. One of several existing model-averaging techniques [6-10] is used to obtain the frequency characteristics of the converter. The results obtained by averaging are known to provide a good approximation only
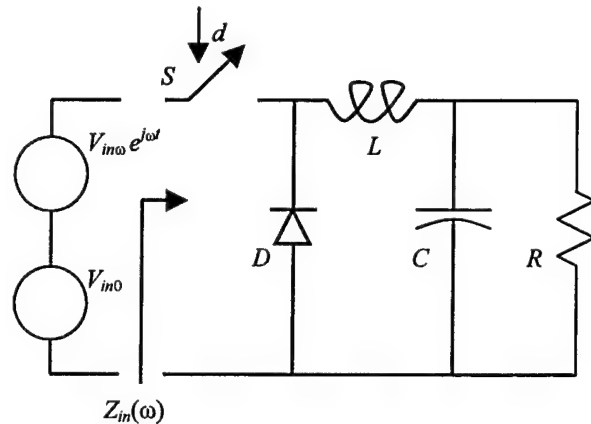

Fig. 1. Switching buck converter with a periodic input and a resistive load.

at frequencies that are significantly below the switching frequency, although certain corrections can be made to the technique to improve its accuracy [10].

The second approach to characterizing converter impedances relies on empirical methods. The most direct of such methods is physical testing using a constant source (or a fixed frequency source for ac systems) and a variable frequency sinusoidal source along with a means for measuring terminal voltages and currents of the converter at various frequencies. The constant source is used to supply the "base-line" power for the converter, while the variable-frequency source is swept over the frequency interval of interest, so that the relationship between the complex values of the input (or output) voltage and current at each frequency can be determined. This method of frequency characterization can also be applied in a computer simulation of the converter.

While the empirical methods can provide accurate impedance characteristics over a wide range of frequencies, these methods are typically very labor-intensive and/or time-consuming. Also, since the results are obtained for a non-LTI (linear time-invariant) system, their usefulness for the Nyquist criterion or other stability analysis techniques for LTI systems is not clear. On the other hand, the results of

linearized model analysis only guarantee the stability of that model, while the actual system can be unstable in some cases even when the model is stable [10].

In this paper, a method of exact calculation of frequency characteristics of outputs for piecewise-LTI periodic systems with periodic inputs is introduced. The idea of the method is analogous to that in [11-13]. The method can be applied to any switching converter model in continuous conduction mode (CCM) that is comprised of ideal switches, ideal diodes, and linear components, with fixed duty cycle ratios of all switches. To illustrate the suggested method, in Section II we use an example of a switching buck converter with constant resistive load (Fig. 1) operating in CCM. This converter represents a typical (although somewhat simplified) load in a distributed power system. The general description of the method that can be applied to any piecewise-LTI periodic system can be found in the Appendix. As our experience has shown, however, formulae (A.9) and (A.17) are more suited for computer treatment rather than human analysis, and compact symbolic results for simple systems can often be obtained faster by analyzing a particular system, as in Section II. In Section III we compare the results of the new method to those obtained using averaging methods and time-domain simulation.

II. ALGORITHM DESCRIPTION

In order to find the frequency dependent input impedance of the converter shown in Fig. 1, we consider the input voltage to be comprised of a dc component and a complex sinusoidal component

$$V_{in} = V_{in0} + V_{in\omega} e^{j\omega t}, \qquad (1)$$

where the first term V_{in0} is the dc or time-independent part, which is included for generality but, as will be seen later, does not affect the final result; the second term is the sinusoidal component that varies with an arbitrary frequency ω and has a constant amplitude $V_{in\omega}$ which may be complex. We define the input impedance of the converter as

$$Z_{in}(\omega) = \frac{V_{in}(\omega)}{I_{in}(\omega)} = \frac{V_{in\omega}}{I_{in}(\omega)}, \qquad (2)$$

where $I_{in}(\omega)$ is the frequency component of the input current at frequency ω, which will be calculated by means of standard Fourier analysis applied to the exact time-domain solution of the state-space model of the circuit. With the assumption that all components of the converter are ideal, the state-space model can be expressed by

$$\frac{d}{dt}\begin{bmatrix} I_L(t) \\ V_C(t) \end{bmatrix} = \begin{bmatrix} 0 & -\frac{1}{L} \\ \frac{1}{C} & -\frac{1}{RC} \end{bmatrix} \cdot \begin{bmatrix} I_L(t) \\ V_C(t) \end{bmatrix} + \begin{bmatrix} \frac{1}{L} \\ 0 \end{bmatrix} \cdot V_{in}'(t) \quad (3)$$

To reflect the switching behavior of the circuit, input to this model is taken to be not V_{in} but a modified input voltage $V_{in}'(t)$ that is defined to be

$$V_{in}'(t) = \begin{cases} V_{in}(t) & nT \le t \le (n+d)T \\ 0 & otherwise \end{cases}, n \in N \quad (4)$$

It is worthwhile to note that this simplification is possible only due to the particular topology of the buck converter. In general, switching cannot be entirely moved into the inputs of the system. The exact time-domain solution of the state-space model, however, can still be found, as shown in the Appendix.

The solution of (3) for each time interval where $V_{in}'(t)$ is a continuous function can be found as a sum of the response forced by $V_{in}'(t)$ and the solution of the homogeneous system with $V_{in}'(t) = 0$. This latter solution can be expressed for the inductor current variable as

$$I_{L0}(t) = C_1 e^{\alpha_1 t} + C_2 e^{\alpha_2 t}, \qquad (5)$$

where

$$\alpha_{1,2} = -\frac{1}{2RC} \pm \sqrt{\frac{1}{4R^2C^2} - \frac{1}{LC}} \qquad (6)$$

and the constants C_1 and C_2 are determined from the initial conditions for the time interval under consideration. Because the system (3) is linear, the complete response can be found as a sum of the transient response (5) due to the initial conditions and the responses forced by the input voltage over each switching cycle. Once the part of the n-th cycle when $V_{in}'(t) \ne 0$ is complete, the forced response of the system due to this cycle can be described by the same expression (5). The constants C_1 and C_2 are now determined by the values of the state variables at the moment $(n+d)T$ that are due to $V_{in}'(t)$ action during the first part of the cycle.

This approach allows us to obtain an expression for the input current $I_{in}(t)$, which is defined as

$$I_{in}(t) = \begin{cases} I_L(t) & nT \le t \le (n+d)T \\ 0 & otherwise \end{cases} \qquad (7)$$

The expression for this current that we get is a finite series of terms that represent contributions from the initial conditions and from each switching cycle prior to the current time t, including the cycle that contains t. Once the series form of $I_{in}(t)$ has been established, the integral Fourier transform is applied to find the component of the current at the desired frequency ω. Finally, (2) is used to determine the input impedance of the converter, which was found to be

$$Z_{in}(\omega) = \frac{\omega L\left[\left(\dfrac{1}{\omega L} - \omega C\right)^2 + \dfrac{1}{R^2}\right]}{d \cdot \Omega_1(\omega) + \Omega_2(\omega, T)}, \qquad (8)$$

where

$$\Omega_1(\omega) = \frac{1}{\omega L R} + j\left[\left(\frac{1}{\omega L} - \omega C\right)\omega C - \frac{1}{R^2}\right]$$

$$\Omega_2(\omega, T) = \frac{C}{(\alpha_2 - \alpha_1)T}\left[\alpha_1 \gamma_2 \Theta(\alpha_2) - \alpha_2 \gamma_1 \Theta(\alpha_1)\right]$$

$$\qquad\qquad\qquad\qquad\qquad\qquad\qquad (9)$$

$$\gamma_{1,2}(\omega) = \frac{\alpha_{2,1}}{\omega L} + \alpha_{1,2}\omega C - j\left[\left(\frac{1}{\omega L} - \omega C\right)\omega + \frac{\alpha_{2,1}}{R}\right]$$

$$\Theta(\alpha_{1,2}) = \frac{\left(1 - e^{(j\omega - \alpha_{1,2})dT}\right)\left(1 - e^{(j\omega - \alpha_{1,2})(1-d)T}\right)}{\left(j\omega - \alpha_{1,2}\right)\left(1 - e^{(j\omega - \alpha_{1,2})T}\right)}$$

Expression (8) permits direct calculation of the input impedance of a buck converter operating in continuous conduction mode at any particular frequency ω, given the essential parameters of the converter, that is, L, C, R, T, and d.

It is interesting to compare (8) to the expression for the input impedance obtained from the state-space averaged model [1] of the buck converter, which is

$$Z_{in_{av}}(\omega) = \frac{\omega L\left[\left(\dfrac{1}{\omega L} - \omega C\right)^2 + \dfrac{1}{R^2}\right]}{d^2 \cdot \Omega_1(\omega)}. \qquad (10)$$

This expression can be obtained from (8) by taking the limit $T \to 0$ (which corresponds to infinite switching frequency), as that leads to $\Omega_2(\omega, T) \to -d(1-d)\Omega_1(\omega)$.

III. VERIFICATION

As a point of comparison between the impedance computed using the new method and using averaging, the input impedance of the circuit in Fig. 1 was computed by both methods over the frequency range from 10 to 10^5 rad/sec. In addition, two time-domain simulations of the same circuit were performed using MATLAB: one with the assumption that the diode and switch were ideal and the other using more realistic models [13-14] for these devices. The following parameter values were used for comparison: $C = 200\ \mu F$, $L = 100\ \mu H$, $R = 2\ \Omega$, $d = 0.375$, $T = 100\ \mu s$, with a resulting switching frequency $\omega_{sw} = \dfrac{2\pi}{T} \approx 6.28 \cdot 10^4$ rad/sec.

Bode plots of the resulting impedances are shown in Fig. 2, where Fig. 2(a) is based on the data obtained by the new
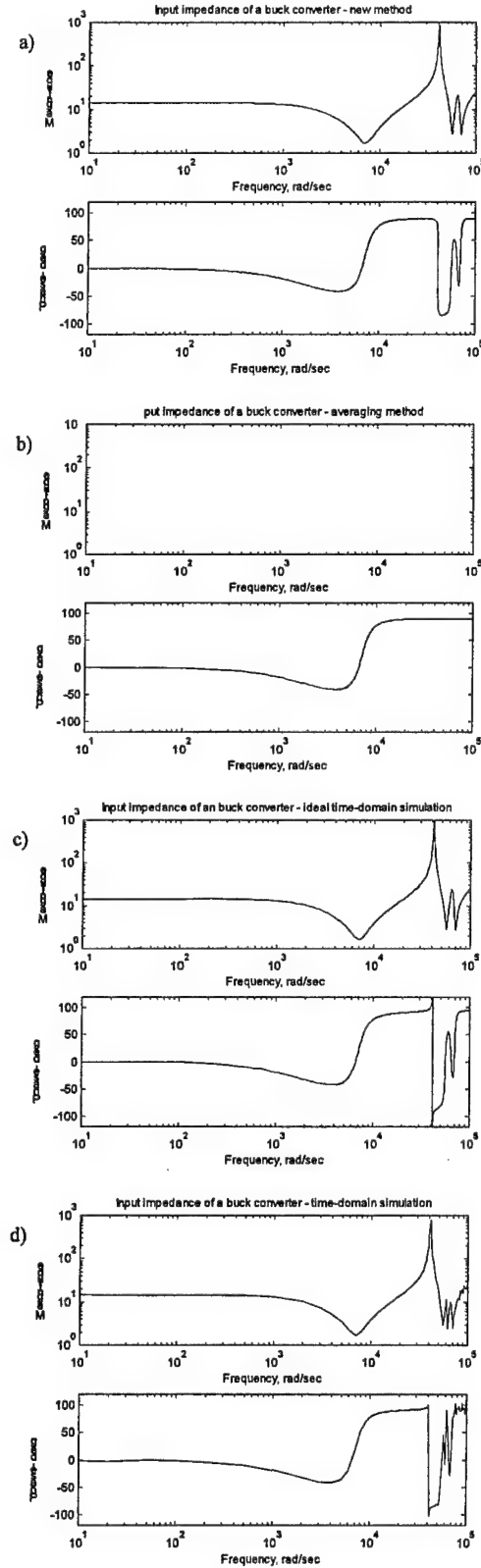

Fig. 2. Buck converter input impedance obtained by: (a) new method; (b) averaging; (c) ideal time-domain simulation; (d) simulation with realistic device models.

approach and Fig. 2(b) on the data that were obtained using state-space averaging. Fig. 2(c) and (d) represent the results of time-domain simulations, with ideal and realistic device models, respectively. It can be seen from the first two plots that at low frequencies the input impedances calculated both from (8) and from (10) are very close to each other. As the frequency increases towards the switching frequency, however, the averaged model fails to predict the correct behavior of the buck converter. The impedance predicted by the new method is shown to be very close to that obtained via simulation, although there are some small differences that are likely due to computational errors and non-idealities included in the more realistic device models.

Although the frequency interval where there is a significant difference between the impedance computed using the new method and the well-established averaged model lies outside of the scope considered in most current applications, we believe that the new approach nevertheless can be useful for stability analysis. While most systems do not operate at the frequencies close to or above the switching frequency, the results in this region may still be important in some cases for the overall stability of the system. The suggested method allows one to calculate impedances and other related characteristics for the actual (non-linearized) system at all frequencies quickly and accurately, which provides an exact estimate of accuracy for the results obtained using averaging and other approximation techniques. Not only the new method is much faster than time-domain simulation; it also yields symbolic expressions for system characteristics, which can be very useful for subsequent analysis.

IV. CONCLUSIONS

The suggested method of exact calculation of input and output impedances for power converter systems provides a new tool for fast and accurate frequency characterization of such systems as an alternative to physical testing and time-domain simulation. The results can be used for stability analysis, as well as for evaluation of the error that is introduced by using averaging techniques.

REFERENCES

[1] R.D. Middlebrook "Input filter considerations in design and application of switching regulators," *Proc. IEEE Industrial Applications Society Annual Meeting*, 1976.

[2] C.M. Wildrick, F.C. Lee "A method of defining the load impedance specifications for a stable distributed power system," *IEEE Transactions on Power Electronics*, vol. 10, no. 3, 1995, pp. 280-285.

[3] X. Feng, Z. Ye, K. Xing, F.C. Lee, D. Borojevic "Individual load impedance specification for a stable DC distributed power system," *IEEE APEC Proceedings*, vol. 2, 1999, pp. 889-894.

[4] S.D. Sudhoff, S.F. Glover, P.T. Lamm, D.H. Schmucker, and D.E. Delisle "Admittance space stability analysis of power electronic systems," *IEEE Transactions on Aerospace and Electronic Systems*, vol. 36, no. 3, 2000, pp. 965-973.

[5] J.G. Kassakian, M.F. Schlecht, and G.C. Verghese, *Principles of Power Electronics*, Addison-Wesley, 1991.

[6] R.D. Middlebrook and S. Cuk "A general unified approach to modeling switching-converter power stages," *International Journal of Electronics*, vol. 42, no. 6, 1976, pp. 521-550.

[7] D.J. Shortt and F.C. Lee "Improved switching converter model using discrete and averaging techniques," *IEEE Transactions on Aerospace and Electronic Systems*, vol. 19, no. 2, 1983, pp. 190-201.

[8] P.T. Krein, J. Bentsman, R.M. Bass, and B.L. Lesieutre "On the use of averaging for the analysis of power electronic systems," *IEEE Transactions on Power Electronics*, vol. 5, no. 2, 1990, pp. 182-190.

[9] S.R. Sanders, J.M. Noworolski, X.Z. Liu, and G.C. Verghese "Generalized averaging method for power conversion circuits," *IEEE Transactions on Power Electronics*, vol. 6, no. 2, 1991, pp. 251-259.

[10] B. Lehman and R.M. Bass "Switching frequency dependent averaged models for PWM DC-DC converters," *IEEE Transactions on Power Electronics*, vol. 11, no. 1, 1996, pp. 89-98.

[11] M.L. Liou "Exact analysis of linear circuits containing periodically operated switches with applications," *IEEE Transactions on Circuit Theory*, vol. 19, no. 2, 1972, pp. 146-154.

[12] T. Strom and S. Signell "Analysis of periodically switched linear circuits," *IEEE Transactions on Circuits and Systems*, vol. 24, no. 10, 1977, pp. 531-541.

[13] R. Tymerski "Exact input-to-output frequency response of time interval modulated switched networks," *IEEE PESC Proceedings*, 1997, pp. 428-434.

[14] P.O. Lauritzen and C.L. Ma "A simple diode model with reverse recovery," *IEEE Transactions on Power Electronics*, vol. 6, no. 2, 1991, pp. 188-191.

[15] A.J. Hefner, Jr. and D.M. Diebolt "An experimentally verified IGBT model implemented in the Saber circuit simulator," *IEEE PESC Proceedings*, vol. 1, 1991, pp. 10-19.

APPENDIX

Consider a system:

$$\begin{cases} \dfrac{dx}{dt} = A(t)x + B(t)u \\ y = C(t)x + D(t)u \end{cases}, t \geq 0, x(0) = x_0, \qquad (A.1)$$

where x, u, and y are vector variables, and matrices $C(t)$ and $D(t)$ are periodic with period T.

We need to find the response of the outputs at a certain frequency ω. We define this response as

$$y(\omega) = \lim_{\tau \to \infty} \frac{1}{\tau} \int_0^\tau y(t)e^{-j\omega t} dt = \\ = \frac{1}{T} \lim_{N \to \infty} \frac{1}{N} \sum_{n=0}^{N-1} \int_{nT}^{(n+1)T} y(t)e^{-j\omega t} dt \qquad (A.2)$$

Here we assume that all integrals and limits exist, which will always be true in case of a stable system. The values of T and ω do not have to be related in any way; ω will be associated with the input vector u which we presume to be independent but known.

Let us assume that we can find the following representation for $x(t)$ when $nT \leq t \leq (n+1)T$:

$$x(t) = \Phi(t - nT)x(nT) + K^+(t - nT)e^{j\omega nT} + \\ + K^-(t - nT)e^{-j\omega nT} + O(t - nT) \qquad (A.3)$$

where matrices Φ, K^+, K^-, and O are all functions of $t-nT$, but not t or n separately.

Applying (A.3) consecutively at each switching cycle, we get:

$$x(nT) = \Phi^n(T)x_0 + \sum_{m=1}^{n}\Phi^{m-1}(T)\times$$

$$[K^+(T)e^{j\omega(n-m)T} + K^-(T)e^{-j\omega(n-m)T} + O(T)] \quad (A.4)$$

Substituting (A.1), (A.3), and (A.4) into (A.2), we obtain the following expression for $y(\omega)$:

$$y(\omega) = y_1(\omega) + y_2(\omega) + y_3(\omega) + y_4(\omega) + \\ + y_5(\omega) + y_6(\omega) + y_7(\omega) + U_\omega \quad (A.5)$$

where

$$y_1(\omega) = \Phi_\omega \lim_{N\to\infty}\left(\frac{1}{N}\sum_{n=0}^{N-1}e^{-j\omega nT}\Phi^n(T)\right)x_0$$

$$y_2(\omega) = \Phi_\omega \lim_{N\to\infty}\left(\frac{1}{N}\sum_{n=0}^{N-1}\sum_{m=1}^{n}\Phi^{m-1}(T)e^{-j\omega mT}\right)K^+(T)$$

$$y_3(\omega) = \Phi_\omega \times \\ \lim_{N\to\infty}\left(\frac{1}{N}\sum_{n=0}^{N-1}e^{-2j\omega nT}\left(\sum_{m=1}^{n}\Phi^{m-1}(T)e^{j\omega mT}\right)\right)K^-(T)$$

$$y_4(\omega) = \Phi_\omega \lim_{N\to\infty}\left(\frac{1}{N}\sum_{n=0}^{N-1}e^{-j\omega nT}\sum_{m=1}^{n}\Phi^{m-1}(T)\right)O(T) \quad (A.6)$$

$$y_5(\omega) = \lim_{N\to\infty}\left(\frac{1}{N}\sum_{n=0}^{N-1}1\right)K_\omega^+$$

$$y_6(\omega) = \lim_{N\to\infty}\left(\frac{1}{N}\sum_{n=0}^{N-1}e^{-2j\omega nT}\right)K_\omega^-$$

$$y_7(\omega) = \lim_{N\to\infty}\left(\frac{1}{N}\sum_{n=0}^{N-1}e^{-j\omega nT}\right)O_\omega$$

and

$$\left[\Phi_\omega, K_\omega^+, K_\omega^-, O_\omega\right] = \\ = \frac{1}{T}\int_0^T C(t)\left[\Phi(t), K^+(t), K^-(t), O(t)\right]e^{-j\omega t}dt$$

$$\left[\tilde{\Phi}(T), \tilde{K}^+(T), \tilde{K}^-(T), \tilde{O}(T)\right] = \\ = \left[\Phi(T), K^+(T), K^-(T), O(T)\right]e^{-j\omega T} \quad (A.7)$$

$$U_\omega = \frac{1}{T}\lim_{N\to\infty}\frac{1}{N}\sum_{n=0}^{N-1}\int_{nT}^{(n+1)T}D(t)u(t)e^{-j\omega t}dt$$

Let us assume that

$$\lim_{N\to\infty}\Phi^N(T) = 0, \quad (A.8)$$

which will be true for any asymptotically stable system.

By calculating the limits in (A.5), we get:

$$y(\omega) = S_1 + \Phi_\omega\left(I - \tilde{\Phi}(T)\right)^{-1}S_2 + U_\omega$$

$$\begin{cases}S_1 = K_\omega^+ \\ S_2 = \tilde{K}^+(T)\end{cases} \text{ if } \omega \neq \frac{\pi k}{T}, k \in Z$$

$$\begin{cases}S_1 = K_\omega^+ + K_\omega^- \\ S_2 = \tilde{K}^+(T) + \tilde{K}^-(T)\end{cases} \text{ if } \omega = \frac{\pi(2k+1)}{T} \quad (A.9)$$

$$\begin{cases}S_1 = K_\omega^+ + K_\omega^- + O_\omega \\ S_2 = \tilde{K}^+(T) + \tilde{K}^-(T) + \tilde{O}(T)\end{cases} \text{ if } \omega = \frac{2\pi k}{T}$$

This result can be applied to an arbitrary piecewise-LTI periodic system, that is, a system of the form:

$$\begin{cases}\dfrac{dx}{dt} = A_\ell x + B_\ell u \\ y = C_\ell x + D_\ell u\end{cases}, (n+d_{\ell-1})T \leq t \leq (n+d_\ell)T \quad (A.10)$$

$$\ell = 1..L; \ A_\ell, B_\ell, C_\ell, D_\ell, d_\ell = const$$

where we assume the inputs to be periodic signals with frequency ω:

$$u = u_0 + F_\ell e^{j\omega t}; u_0, F_\ell = const. \quad (A.11)$$

We need to find the representation (A.3) for the state variable vector x, then we can use (A.9) to calculate $y(\omega)$.

Let us use the following definitions:

$$[\tilde{\Phi}_\ell, \tilde{K}_\ell^+, \tilde{K}_\ell^-, \tilde{O}_\ell] = [\Phi(t-nT), K^+(t-nT), \\ K^-(t-nT), O(t-nT)]\cdot e^{-j\omega(t-nT)} \quad (A.12)$$

Here the variables on the left side are also all functions of $t-nT$, and the index ℓ designates the time interval $(n+d_{\ell-1})T \leq t \leq (n+d_\ell)T$ where they are defined. Since the parameters in the state-space model (A.10) are different for different values of ℓ, it is necessary to consider each time interval separately. During each interval, (A.10) describes a linear time-invariant system, so we can use the well-known solution for x from linear systems theory [5]:

$$x(t) = e^{A(t-t_0)}\cdot x(t_0) + \int_{t_0}^{t}e^{A(t-\tau)}Bu(\tau)d\tau, \quad (A.13)$$

where $A = A_\ell; B = B_\ell; t_0 = (n+d_{\ell-1})T$. Using mathematical induction, it can be shown that in case of the input (A.11), the functions defined by (A.12) can be calculated as

$$\tilde{\Phi}_\ell = e^{A_{\ell\omega}[t-(n+d_{\ell-1})T]}\cdot\prod_{i=1}^{\ell-1}\Psi_{i\omega}$$

$$\tilde{K}_\ell^+ = A_{\ell\omega}^{-1}\left\{e^{A_{\ell\omega}[t-(n+d_{\ell-1})T]} - I\right\}B_\ell F_\ell + e^{A_{\ell\omega}[t-(n+d_{\ell-1})T]}\times \\ \sum_{j=1}^{\ell-1}\left\{\left(\prod_{i=j+1}^{\ell-1}\Psi_{i\omega}\right)A_{j\omega}^{-1}\left(\Psi_{j\omega} - I\right)B_j F_j\right\}$$

$$\tilde{K}_\ell^- = 0 \qquad (A.14)$$

$$\tilde{O}_\ell = e^{-j\omega(t-nT)}\left\{ \begin{array}{l} A_\ell^{-1}\left(e^{A_\ell[t-(n+d_{\ell-1})T]} - I\right)B_\ell u_0 + \\ e^{A_\ell[t-(n+d_{\ell-1})T]}\sum_{j=1}^{\ell-1}\left[\left(\prod_{i=j+1}^{\ell-1}\Psi_i\right)A_j^{-1}\left(\Psi_j - I\right)B_j u_0\right] \end{array}\right\}$$

where

$$\begin{aligned} A_{\ell\omega} &= A_\ell - j\omega I \\ \Delta_\ell &= d_\ell - d_{\ell-1} \\ \Psi_\ell &= e^{A_\ell\Delta_\ell T} \\ \Psi_{\ell\omega} &= e^{A_{\ell\omega}\Delta_\ell T} \end{aligned} \qquad (A.15)$$

Here I is the identity matrix and all products (Π) are taken so that the terms with higher indices are applied from the left side, that is,

$$\left(\prod_{\ell=1}^L \Psi_\ell\right) = \Psi_L \cdot \Psi_{L-1} \cdot \ldots \cdot \Psi_1, \qquad (A.16)$$

etc. Also, if the upper index of a sum (product) has a smaller value than the lower index, that is, if the sum (product) contains no terms, then the value of such empty sum (product) is assumed to be zero (unity).

Using (A.7), (A.10), (A.11), and (A.14), we finally get:

$$U_\omega = \begin{cases} \sum_{l=1}^L D_\ell F_\ell \Delta_\ell, & \text{if } \omega \neq \dfrac{2\pi k}{T} \\ \sum_{l=1}^L D_\ell [F_\ell \Delta_\ell + \dfrac{j}{\omega T}u_0 \times \\ \quad (e^{-j\omega d_\ell T} - e^{-j\omega d_{\ell-1}T})], & \text{if } \omega = \dfrac{2\pi k}{T} \end{cases}$$

$$\tilde{\Phi}(T) = \prod_{\ell=1}^L \Psi_{\ell\omega} \qquad (A.17)$$

$$\tilde{K}^+(T) = \sum_{\ell=1}^L \left\{\left(\prod_{i=\ell+1}^L \Psi_{i\omega}\right)A_{\ell\omega}^{-1}\left(\Psi_{\ell\omega} - I\right)B_\ell F_\ell\right\}$$

$$\tilde{K}^-(T) = 0$$

$$\tilde{O}(T) = \sum_{\ell=1}^L \left\{\left(\prod_{i=\ell+1}^L \Psi_i\right)A_\ell^{-1}\left(\Psi_\ell - I\right)B_\ell u_0\right\} \cdot e^{-j\omega T}$$

$$\Phi_\omega = \frac{1}{T}\sum_{\ell=1}^L \left\{C_\ell A_{\ell\omega}^{-1}\left(\Psi_{\ell\omega} - I\right)\left(\prod_{i=1}^{\ell-1}\Psi_{i\omega}\right)\right\} \qquad \begin{array}{l}(A.17)\\ \text{continued}\end{array}$$

$$K_\omega^+ = \frac{1}{T}\sum_{\ell=1}^L \left\{C_\ell A_{\ell\omega}^{-1}\left\langle\left(\Psi_{\ell\omega} - I\right)Q_1 - TB_\ell F_\ell \Delta_\ell\right\rangle\right\}$$

$$K_\omega^- = 0$$

$$O_\omega = \frac{1}{T}\sum_{\ell=1}^L \left\{C_\ell e^{-j\omega d_{\ell-1}T}\left\langle A_{\ell\omega}^{-1}\left(\Psi_{\ell\omega} - I\right)Q_2 - Q_3\right\rangle\right\}$$

where

$$Q_1 = A_{\ell\omega}^{-1}B_\ell F_\ell + \sum_{i=1}^{\ell-1}\left(\prod_{m=i+1}^{\ell-1}\Psi_{m\omega}\right)A_{i\omega}^{-1}\left(\Psi_{i\omega} - I\right)B_i F_i$$

$$Q_2 = A_\ell^{-1}B_\ell u_0 + \sum_{i=1}^{\ell-1}\left(\prod_{m=i+1}^{\ell-1}\Psi_m\right)A_i^{-1}\left(\Psi_i - I\right)B_i u_0 \quad (A.18)$$

$$Q_3 = A_\ell^{-1}\frac{j}{\omega}\left(e^{-j\omega\Delta_\ell T} - 1\right)B_\ell u_0$$

Using (A.9) and (A.17), the exact frequency components of the outputs of the piecewise-LTI periodic system (A.10) at a given frequency ω of the input signal can be readily obtained. For a power converter system with ideal switches and diodes, assigning the unknown terminal voltages and/or currents to be the outputs of the model (A.10), input and output impedances can then be calculated using (2).

APPENDIX **C**

Stability of Periodic Solutions
for Multi-Topology DC-to-DC Power Converters

S. G. Kriventsov and J. S. Mayer
Department of Electrical Engineering
The Pennsylvania State University
121 EE East
University Park, PA 16802

Abstract - An analytical nonlinear technique is developed for stability analysis of periodic solutions for dc-to-dc power converter systems with multiple independently controlled switches and possible discontinuous topologies. The new approach, based on discrete nonlinear maps, is exact under the assumption of ideal switches and is easily programmable, which allows for nearly instantaneous evaluation of stability of periodic solutions for dc power systems under a wide range of input conditions. The results obtained using the new method were in agreement with those acquired using much slower time-domain simulation method. The exactness of the new method is a definite advantage over existing linear methods and other approximate techniques.

I. INTRODUCTION

There have been numerous papers [1-4] devoted to the stability analysis of dc-to-dc power converters and systems constructed by interconnecting such converters. Until recently, most of these papers used state-space averaging [1-3, 5] or other approximate linear methods [4] to simplify the problem. Such methods, while widely used, are not guaranteed to provide a correct assessment of stability for the actual nonlinear power system. Consequently, circuit designers often resort to unduly conservative choices to ensure adequate stability margins. Another popular practical method of stability analysis of power systems is by means of numerical time-domain simulation, using either specialized simulators that are available commercially or general-purpose software packages such as MATLAB. Time-domain simulation provides a simple means for stability assessment of a system with known inputs and parameters, along with the additional benefit of accommodating arbitrarily realistic models for switching devices and other system components, but there are also significant drawbacks to such analysis. Simulating a system for a large number of different input conditions or system parameters can be very time consuming, and the presence of instability may not be immediately obvious on a short time scale, thus requiring longer simulations. Moreover, numerical errors may accumulate over many switching cycles, making the result of the simulation somewhat less reliable.

In recent years, several authors have applied exact nonlinear analysis methods to dc switching converter systems [6, 7]. For such analysis, a mapping function (also called a Poincaré map) can be defined that is basically a transition function for the state variables of the system over a switching cycle that includes changes due to external inputs. In the normal mode of operation of such systems, there exists a periodic solution (a fixed point of the mapping), that is, a point in the state space that repeats itself after each switching cycle. The asymptotic stability of such solution can be defined as its ability to attract points that are sufficiently close to it, which means that in the case of a small perturbation the trajectory will eventually approach the periodic orbit. A more rigorous definition of stability can be found in [8].

To assess the stability of periodic solutions, Floquet theory for periodic systems can be used [6, 8]. In the present paper, the method employed in [6] is developed for systems with multiple topologies that can exist due to several independently controlled switches and/or presence of

discontinuous modes [9] in the system. Explicit closed-form expressions for the characteristic (Floquet) multipliers of a periodic solution for all such systems are obtained in Section II. These expressions can be readily used in computer analysis without requiring time-consuming numerical simulations. In Section III, two typical examples of power systems are analyzed using the new approach. The same systems are also analyzed using time-domain simulation, and the results are compared to show the validity and advantages of the new method.

II. ANALYSIS

Let us consider a general piecewise-LTI (linear time-invariant) system with constant inputs:

$$\frac{dx}{dt} = A(t)x + B(t)u, u = const$$

$$\begin{cases} A(t) = A_m = const \\ B(t) = B_m = const \end{cases} \text{when } d_{m-1}^k T \le t - kT \le d_m^k T \quad (1)$$

$$m = 1..N; 0 \le d_m^k \le 1$$

where x and u are column vectors. The integer variable k is the switching cycle number, T is the switching period, and N is the number of circuit topologies that the system goes through during one cycle. The value of each d_m^k defines the instant $d_m^k T$ counted from the beginning of the kth switching cycle when the system is switched from m^{th} to $(m+1)^{st}$ topology during that cycle. Matrices A and B are assumed to be independent of k. By definition we set $d_0^k = 0, d_N^k = 1$ for all values of k, which means that k^{th} switching cycle starts at $t = kT$ and ends at $t = (k+1)T$. All the other d_m^k values are determined dynamically during each cycle due to the state feedback controls and/or presence of discontinuous modes.

Let us assume first that all switching instants d_m^k for the kth cycle are known. Defining x_m^k to be the value of the state-variable vector x of the system during the mth switching

instant of the kth cycle, that is, $x_m^k = x[(k + d_m^k)T]$, and using results from linear systems theory, we get the following expression for x_1^k:

$$x_1^k = \Phi_1^k x_0^k + \Psi_1^k B_1 u \quad (2)$$

where we introduced notation

$$\Delta_m^k = d_m^k - d_{m-1}^k; \quad \Phi_m^k = e^{A_m \Delta_m^k T}$$

$$\Psi(A, t) = \int_0^t e^{A\tau} d\tau = It + \frac{At^2}{2!} + \frac{A^2 t^3}{3!} + ... ; \quad (3)$$

$$\Psi_m^k = \Psi(A_m, \Delta_m^k T)$$

Here I is the identity matrix of the same size as A. Notice that $A_m \Psi_m^k + I = \Phi_m^k$. If matrix A_m is invertible then $\Psi_m^k = A^{-1}(\Phi_m^k - I)$.

Now, taking x_1^k as a new initial value for the second time interval $(k + d_1^k)T \le t \le (k + d_2^k)T$, and using the same method for all the remaining topologies, we obtain the following exact expression for the state-variable vector of the system at the end of the switching cycle:

$$x_0^{k+1} = x_N^k = f(x_0^k, d_1^k, ..., d_N^k, u)$$
$$= \Pi_1^N x_0^k + E_N^k u \quad (4)$$

where Π_p^q stands for the following matrix product:

$$\Pi_p^q = \prod_{i=p}^q \Phi_i^k = \Phi_q^k \cdot \Phi_{q-1}^k \cdot ... \cdot \Phi_p^k \quad (5)$$

and $E_q^k = \sum_{i=1}^q \Pi_{i+1}^q \Psi_i^k B_i$. Equation (4) provides an exact expression for the Poincaré map of the system, assuming that all switching instants are known. In this paper, we are interested in the stability of periodic orbits of the system, that is, solutions that satisfy the condition $x_0^{k+1} = x_0^k = x_0$, which means that x_0 is a fixed point of the mapping. Such

9999

solutions are periodic with period T, since we assume that the topologies and the form of switching conditions do not change from one cycle to another.

From (4), we find that if $\det\left(I - \Pi_1^N\right) \neq 0$, which is often the case, there is always exactly one fixed point for the given values of switching instants, which is $x_0 = \left(I - \Pi_1^N\right)^{-1} E_N^k u$. In practical systems, the equations for the switching instants d_m^k, which are defined by the control method and contain x_0 as a parameter, must be solved together with (4) to find the actual values of d_m^k and x_0. Typically, the complicated nature of switching conditions does not allow an analytical solution, so this must be done numerically. For the rest of this paper, we will assume that the fixed point x_0 is known, and we will investigate the stability of the orbit defined by it.

In our analysis we will use Floquet theory [6, 8]. According to this theory, if we define D_m and U to be respectively the values of the switching instants and the inputs for our periodic solution, and introduce small perturbations:

$$x_0^k = x_0 + \hat{x}^k, \quad d_m^k = D_m + \hat{d}_m^k, \quad u = U + \hat{u} \qquad (6)$$

the periodic orbit defined by x_0 will be stable if and only if the eigenvalues of the matrix H_1 in the first order expansion

$$\hat{x}^{k+1} = H_1 \hat{x}^k + H_2 \hat{u} \qquad (7)$$

all lie within the unit circle in the complex plane. Thus, computation of the eigenvalues of H_1 provides a conclusion about the stability of the periodic solution.

Let us consider the following form of switching condition:

$$\sigma_m\left(x_0^k, d_1^k, d_2^k, ..., d_m^k, u\right) = \varphi_m \cdot x\left[\left(k + d_m^k\right)T\right] + V_m d_m^k + C_m + P_m u = 0 \qquad (8)$$

Here $m = 1..N - 1$; φ_m is a constant vector that defines which state variables will be used to determine the mth switching instant, while V_m, C_m, and P_m are scalar constants for each m that are employed to adapt (8) for different cases of switching. The condition of the form (8) is quite general, as it can be used to describe both switching due to PWM controllers (where V_m will be the ramp voltage of the input to the comparator) and transitions into discontinuous modes that occur when one of the state variables reaches a certain value (typically zero), as well as other cases. In the case of discontinuous mode transitions, V_m should be set to zero.

Substituting (6) into (4) and (8), and leaving only the first order terms with respect to perturbations, we obtain:

$$\begin{cases} \hat{x}^{k+1} = \dfrac{\partial f}{\partial x}\hat{x}^k + \dfrac{\partial f}{\partial d_1}\hat{d}_1^k + ... + \dfrac{\partial f}{\partial d_{N-1}}\hat{d}_{N-1}^k + \dfrac{\partial f}{\partial u}\hat{u} \\ 0 = \dfrac{\partial \sigma_1}{\partial x}\hat{x}^k + \dfrac{\partial \sigma_1}{\partial d_1}\hat{d}_1^k + \dfrac{\partial \sigma_1}{\partial u}\hat{u} \\ 0 = \dfrac{\partial \sigma_2}{\partial x}\hat{x}^k + \dfrac{\partial \sigma_2}{\partial d_1}\hat{d}_1^k + \dfrac{\partial \sigma_2}{\partial d_2}\hat{d}_2^k + \dfrac{\partial \sigma_2}{\partial u}\hat{u} \\ ... \\ 0 = \dfrac{\partial \sigma_{N-1}}{\partial x}\hat{x}^k + \dfrac{\partial \sigma_{N-1}}{\partial d_1}\hat{d}_1^k + ... + \dfrac{\partial \sigma_{N-1}}{\partial d_{N-1}}\hat{d}_{N-1}^k + \dfrac{\partial \sigma_{N-1}}{\partial u}\hat{u} \end{cases} \qquad (9)$$

Next, we express $\hat{d}_1^k$ from the second equation of (9), substitute it into the third equation and find $\hat{d}_2^k$, and repeat the process until the last equation to find $\hat{d}_m^k$, $m = 1..N$. The following expression valid for all $\hat{d}_m^k$ can be obtained:

$$\hat{d}_m^k = \gamma_m^x \cdot \hat{x}^k + \gamma_m^u \cdot \hat{u}$$

$$\gamma_m^{x(u)} = \sum_{l=0}^{m-1} \sum_{\substack{\alpha_0 > \alpha_1 > ... > \alpha_l \\ \alpha_i = 1...m-1 \\ \alpha_0 = m}} \frac{\dfrac{\partial \sigma_{\alpha_l}}{\partial x(u)} \cdot \prod\limits_{i=0}^{l-1} \dfrac{\partial \sigma_{\alpha_i}}{\partial d_{\alpha_{i+1}}}}{(-1)^{l+1} \prod\limits_{i=0}^{l} \dfrac{\partial \sigma_{\alpha_i}}{\partial d_{\alpha_i}}} \qquad (10)$$

Here the inner summation in the brackets is taken over all the possible combinations of l different integer numbers $\alpha_i, i = 1..l$ such that $m = \alpha_0 > \alpha_1 > ... > \alpha_l > 0$.

Substituting (10) into the first equation of (9), we get an expression of the form (7), where

$$H_1 = \frac{\partial f}{\partial x} + \sum_{m=1}^{N-1} \frac{\partial f}{\partial d_m} \gamma_m^x$$
$$H_2 = \frac{\partial f}{\partial u} + \sum_{m=1}^{N-1} \frac{\partial f}{\partial d_m} \gamma_m^u \qquad (11)$$

By substituting the expressions for γ_m^x and γ_m^u into (11) and rearranging the terms in the summations, the following result for H_1 and H_2 can be obtained:

$$H_1 = \frac{\partial f}{\partial x} + \sum_{l=1}^{N-1} \sum_{\substack{\alpha_1 \succ ... \succ \alpha_l \\ \alpha_i = 1...N-1}} \left[\frac{\frac{\partial f}{\partial d_{\alpha_1}} \cdot \prod_{i=1}^{l} \frac{\partial \sigma_{\alpha_i}}{\partial d_{\alpha_{i+1}}} \cdot \frac{\partial \sigma_{\alpha_l}}{\partial x}}{(-1)^{l+1} \prod_{i=0}^{l} \frac{\partial \sigma_{\alpha_i}}{\partial d_{\alpha_i}}} \right]$$

$$H_2 = \frac{\partial f}{\partial u} + \sum_{l=1}^{N-1} \sum_{\substack{\alpha_1 \succ ... \succ \alpha_l \\ \alpha_i = 1...N-1}} \left[\frac{\frac{\partial f}{\partial d_{\alpha_1}} \cdot \prod_{i=1}^{l} \frac{\partial \sigma_{\alpha_i}}{\partial d_{\alpha_{i+1}}} \cdot \frac{\partial \sigma_{\alpha_l}}{\partial u}}{(-1)^{l+1} \prod_{i=0}^{l} \frac{\partial \sigma_{\alpha_i}}{\partial d_{\alpha_i}}} \right] \qquad (12)$$

Calculating the derivatives in (12), we get:

$$\frac{\partial \sigma_\alpha}{\partial x} = \varphi_\alpha \Pi_1^\alpha; \quad \frac{\partial \sigma_\alpha}{\partial u} = \varphi_\alpha E_\alpha + P_\alpha$$
$$\frac{\partial \sigma_\alpha}{\partial d_\alpha} = \varphi_\alpha T(A_\alpha X_\alpha + B_\alpha U) + V_\alpha$$
$$\frac{\partial \sigma_\beta}{\partial d_\alpha}\bigg|_{\alpha \prec \beta} = \varphi_\beta \Pi_{\alpha+1}^\beta \Gamma_\alpha \qquad (13)$$
$$\frac{\partial f}{\partial x} = \Pi_1^N; \quad \frac{\partial f}{\partial u} = E_N; \quad \frac{\partial f}{\partial d_\alpha} = \Pi_{\alpha+1}^N \Gamma_\alpha.$$

where $X_\alpha = \Pi_1^\alpha x_0 + E_\alpha U$ is the point on the periodic orbit of the system at $t = d_\alpha T$, and we defined $\Gamma_\alpha = T[(A_\alpha - A_{\alpha-1})X_\alpha + (B_\alpha - B_{\alpha-1})U]$. For all variables in (13), we omit the upper index k that we used before for the cycle number since they are now calculated for the periodic orbit and only depend on x_0, D_m, and U, not the perturbations.

The expressions (12), (13) can be easily programmed for automatic calculation of Floquet multipliers for any system of the form (1) with switching conditions as in (8) and a known fixed point x_0.

III. RESULTS

Let us apply the developed method to calculate the Floquet multipliers and thereby assess the stability of two example circuits. All the switches and components of the circuits are assumed to be ideal. The first system that we consider (Fig. 1a on the next page) is a basic buck converter circuit; the second one (Fig. 1b on the next page) is an ARCP (auxiliary resonant commutated pole) circuit [10] featuring four controlled switches. Both circuits are assumed to have constant (dc) inputs.

The chosen circuits are similar in the way that when one of the main switches (S_1 or S_2) of the ARCP circuit is open, the right part of the circuit behaves as a buck converter with an input voltage equal to the voltage across capacitor C_2.

Since the control method is not essential when applying the proposed stability analysis method as long as switching conditions have the form (8), a basic integrator was used to control the output voltage of both circuits to generate the results presented in this section. Similar results were obtained with other controllers, e.g. a lag-lead controller with an integrator as in [6]. However, the increase of the system matrix size in the latter case due to the controller states introduces additional Floquet multiplier values related to the controller dynamics, which makes the results less transparent (although the analysis is the same). Therefore, a simpler controller was chosen for the sake of clarity.
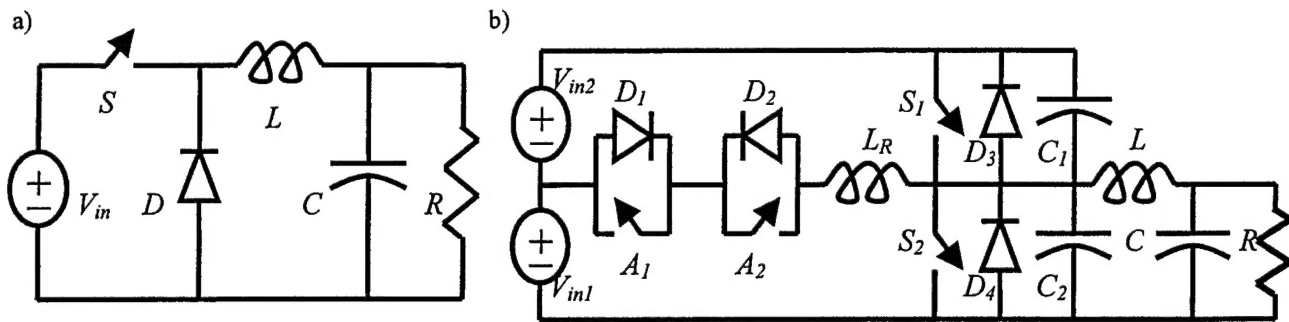
Fig. 1. a) Switching buck converter and b) ARCP circuit, both with a constant input voltage and a resistive load.

For both circuits, the following values were used: $C = 100$ μF, $L = 100$ μH, $R = 18$ Ω. For the ARCP circuit, we also used $C_1 = C_2 = 40$ nF, $L_R = 3.5$ μH. The time constant of the integrator was chosen to be $\tau = 0.4$ sec, and the switching period was $T = 20$ μsec. For both circuits the reference voltage of the controller was chosen to be 150V to produce a dc output of that value. The input voltage for both circuits (V_{in} in Fig. 1a and $2V_{in1}=2V_{in2}$ in Fig. 1b) was varied between 170V and 400V. Due to the nature of the systems, it is necessary for their successful operation that the input voltage be higher than the desired output. For each circuit, periodic solutions were found for all input voltages.

To use the new method, a state-space model was developed for each circuit, and Floquet multipliers were calculated for different input voltages. The maximum absolute value of Floquet multiplier F_{max} as a function of the input voltage is shown in Fig. 2a for the buck converter and Fig. 2b for the ARCP circuit. These data were calculated using the technique described in Section II.

It can be seen from Fig. 2 that, despite the similarity of the circuits, Floquet multiplier values behave differently for these two systems. For the buck converter, the largest multiplier value F_{max}^{buck} increases as a function of the input voltage between 170V and approximately 337.2V. It crosses the value of unity at about 236.1V, which means that between 170V and 236.1V the periodic solutions for the buck
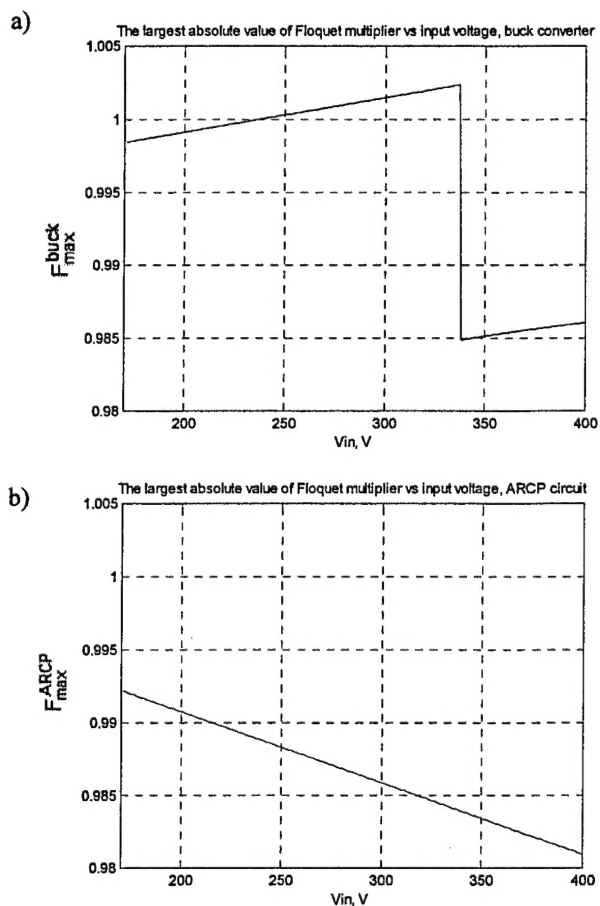

Fig. 2. The largest absolute value of Floquet multiplier vs input voltage for a) buck converter; b) ARCP circuit.

converter are stable, and between 236.1V and 337.2V they are unstable. At 337.2V, due to a transition into discontinuous mode of operation, the value of F_{max}^{buck} falls

9999

abruptly, which results in stable periodic solutions between 337.2V and 400V for the buck converter circuit.

For the ARCP circuit, although the largest Floquet multiplier value F_{max}^{ARCP} is not constant as a function of the input voltage, it can be seen from Fig. 2b that for all the values of the input voltage F_{max}^{ARCP} is well below unity. This means that periodic solutions for the ARCP circuit are stable between 170V and 400V. This result was confirmed by time-domain simulation, as were the results for the buck converter.

The reason for greater stability of the ARCP circuit is the presence of an intrinsic stabilizing mechanism that exists in the system. The switching of the ARCP circuit is discussed in detail in [10]. The first stage of the switching cycle, before the switch S_2 is turned off and the capacitor C_2 starts charging, takes longer if the current through the inductor L is higher, which happens in the case when the voltage across the capacitor C is higher. A longer initial stage reduces the time when C is being charged, thus lowering the voltage across it. Similar argument can be applied for the case when the output voltage is lower than the desired value.

IV. SUMMARY AND CONCLUSION

A new method was developed for exact nonlinear stability analysis of piecewise-LTI switching circuits. This method can be applied to circuits with multiple switches and discontinuous modes. Based on the expressions of the developed approach, a computer program was created that can quickly evaluate the stability of a given periodic solution for a system described by a state-space model. The program was tested on two practical circuits, when the results of analysis were compared against those obtained using numerical simulation. In both cases the stability results obtained using the new method were confirmed by standard techniques. To conclude, the new method provides a fast and accurate way of stability analysis of periodic solutions for power circuits.

REFERENCES

[1] R. D. Middlebrook "Input filter considerations in design and application of switching regulators," *Proc. IEEE Industrial Applications Society Annual Meeting*, 1976.

[2] P.T. Krein, J. Bentsman, R.M. Bass, and B.L. Lesieutre "On the use of averaging for the analysis of power electronic systems," *IEEE Transactions on Power Electronics*, vol. 5, no. 2, 1990, pp. 182-190.

[3] C. M. Wildrick, F. C. Lee "A method of defining the load impedance specifications for a stable distributed power system," *IEEE Transactions on Power Electronics*, vol. 10, no. 3, 1995, pp. 280-285.

[4] B. Lehman and R.M. Bass "Extensions of averaging theory for power electronic systems," *IEEE Transactions on Power Electronics*, vol. 11, no. 4, 1996, pp. 542-553.

[5] R. D. Middlebrook and S. Cuk "A general unified approach to modeling switching converter power stages," *IEEE PESC Proceedings*, 1976, pp. 18-34.

[6] S. K. Mazumder, A. H. Nayfeh, and D. Boroyevich "Theoretical and experimental investigation of the fast- and slow-scale instabilities of a dc-dc converter," *IEEE Transactions on Power Electronics*, vol. 16, no. 2, 2001, pp. 201-216.

[7] C. C. Fang and E. H. Abed "Sampled-data modeling and analysis of the power stage of PWM dc-dc converters," *International Journal of Electronics*, vol. 88, no. 3, 2001, pp. 347-369.

[8] S. Banerjee and G. C. Verghese "Nonlinear phenomena in power electronics," 2001.

[9] N. Femia, G. Spagnuolo, and V. Tucci "State-space models and order reduction for dc-dc switching converters in discontinuous modes," IEEE Transactions on Power Electronics, vol. 10, no. 6, 1995, pp. 640-650.

[10] R.W. De Doncker and J.P. Lyons "The auxiliary resonant commutated pole converter," *Proc. IEEE Industrial Applications Society Annual Meeting*, 1990, pp. 1228-1235.